



Global evaluation of ammonia bidirectional exchange and livestock diurnal variation schemes

L. Zhu¹, D. Henze¹, J. Bash², G.-R. Jeong^{1,2}, K. Cady-Pereira³, M. Shephard⁴, M. Luo⁵, F. Paulot^{6,7}, and S. Capps²

¹Department of Mechanical Engineering, University of Colorado, Boulder, Colorado, USA

²US Environmental Protection Agency, Research Triangle Park, North Carolina, USA

³Atmospheric and Environmental Research, Inc., Lexington, Massachusetts, USA

⁴Environment Canada, Toronto, Ontario, Canada

⁵Jet Propulsion Laboratory, California Institute of Technology Pasadena, CA, USA

⁶Program in Atmospheric and Oceanic Sciences, Princeton University, Princeton, New Jersey, USA

⁷Geophysical Fluid Dynamics Laboratory/National Oceanic and Atmospheric Administration, Princeton, New Jersey, USA

Correspondence to: D. Henze (daven.henze@colorado.edu)

Received: 7 December 2014 – Published in Atmos. Chem. Phys. Discuss.: 20 February 2015

Revised: 10 October 2015 – Accepted: 9 November 2015 – Published: 19 November 2015

Abstract. Bidirectional air–surface exchange of ammonia (NH_3) has been neglected in many air quality models. In this study, we implement the bidirectional exchange of NH_3 in the GEOS-Chem global chemical transport model. We also introduce an updated diurnal variability scheme for NH_3 livestock emissions and evaluate the recently developed MASAGE_ NH_3 bottom-up inventory. While updated diurnal variability improves comparison of modeled-to-hourly in situ measurements in the southeastern USA, NH_3 concentrations decrease throughout the globe, up to 17 ppb in India and southeastern China, with corresponding decreases in aerosol nitrate by up to $7 \mu\text{g m}^{-3}$. The ammonium (NH_4^+) soil pool in the bidirectional exchange model largely extends the NH_3 lifetime in the atmosphere. Including bidirectional exchange generally increases NH_3 gross emissions (7.1 %) and surface concentrations (up to 3.9 ppb) throughout the globe in July, except in India and southeastern China. In April and October, it decreases NH_3 gross emissions in the Northern Hemisphere (e.g., 43.6% in April in China) and increases NH_3 gross emissions in the Southern Hemisphere. Bidirectional exchange does not largely impact NH_4^+ wet deposition overall. While bidirectional exchange is fundamentally a better representation of NH_3 emissions from fertilizers, emissions from primary sources are still underestimated and thus significant model biases remain when compared to in situ measurements in the USA. The adjoint of bidirectional exchange has also been developed for the GEOS-Chem model and is

used to investigate the sensitivity of NH_3 concentrations with respect to soil pH and fertilizer application rate. This study thus lays the groundwork for future inverse modeling studies to more directly constrain these physical processes rather than tuning bulk unidirectional NH_3 emissions.

1 Introduction

Ammonia (NH_3) is an important precursor of particulate matter ($\text{PM}_{2.5}$) that harms human health (Reiss et al., 2007; Pope et al., 2009; Crouse et al., 2012) and impacts climate through aerosol and short-lived greenhouse gas concentrations (Langridge et al., 2012). Global emissions of NH_3 have increased by a factor of 2 to 5 since preindustrial times, and they are projected to continue to rise over the next 100 years (Lamarque et al., 2011; Ciais et al., 2013). NH_3 is an important component of the nitrogen cycle and accounts for a significant fraction of long-range transport (100s of km) of reactive nitrogen (Galloway et al., 2008). Excessive deposition of NH_3 already threatens many sensitive ecosystems (Liu et al., 2013).

Uncertainties in estimates of NH_3 emissions are significant. Surface-level NH_3 measurements have been limited in spatial and temporal coverage, leading to large discrepancies in emissions estimates (Pinder et al., 2006). Additional information from remote sensing observations has

been used to gain a better understanding of NH₃ distributions (Clarisse et al., 2009; Shephard et al., 2011; Pinder et al., 2011; Van Damme et al., 2014). These observations have also been used as inverse modeling constraints on NH₃ emissions (Zhu et al., 2013). While this approach leads to improved results regarding the comparison of air quality model estimates to independent surface observations in the USA (Zhu et al., 2013), several limitations of this approach were identified. First, model biases in NH_x wet deposition were not reduced. Emission constraints from remote sensing measurements available only once per day were very sensitive to the model's diurnal variation of NH₃ sources. Also, the remote sensing observations used in Zhu et al. (2013) are sparsely distributed, leading to a quantifiable sampling bias. Other inverse modeling studies of NH₃ emissions have been performed using in situ observations, such as aerosol SO₄²⁺ and NO₃⁻ (Henze et al., 2009), aircraft observations of NH₃ (Schiferl et al., 2014), or wet deposition of NH₄⁺ (Paulot et al., 2014). However, these approaches still have disadvantages as they are limited to the small spatiotemporal coverage of available aircraft measurements or are sensitive to large model biases in HNO₃ (Heald et al., 2012; Zhang et al., 2012) or precipitation (Paulot et al., 2014).

The modest success of previous inverse modeling studies suggests that updates to the dynamic and physical processes governing NH₃ are needed in addition to improvements in emissions estimates. Nighttime NH₃ concentrations are consistently overestimated in many air quality models (e.g., GEOS-Chem global chemical transport model and the Community Multi-scale Air Quality (CMAQ) model). This may contribute to an overestimate of monthly averaged NH₃ concentration following the assimilation of Tropospheric Emission Spectrometer (TES) observations (Zhu et al., 2013).

Another area in which many air quality models are currently deficient is in treatment of the air–surface exchange of NH₃. Rigorous treatment of the bidirectional flux of NH₃ can substantially impact NH₃ deposition, emission, re-emission, and atmospheric lifetime (Sutton et al., 2007). Re-emission of NH₃ from soils can be a significant part of NH₃ sources in some regions. However, this bidirectional exchange mechanism is neglected by many air quality models (e.g., GEOS-Chem). Several recent studies have begun to include resistance-based bidirectional exchange wherein the NH₃ flux direction is determined by comparing the ambient NH₃ concentration to the NH₃ in-canopy compensation point. Sutton et al. (1998) and Nemitz et al. (2001) began with the air–canopy exchange model and extended the model by including air–soil exchange but with no soil resistance. Cooter et al. (2010) and Bash et al. (2010) developed and extended the model to include a soil capacitance which assumes that NH₃ and NH₄⁺ exist in equilibrium in the soil. This NH₃ bidirectional exchange scheme has been evaluated in a regional air quality model (CMAQ) by Bash et al. (2013) and Pleim et al. (2013).

Based on these previous studies, investigating the diurnal patterns of NH₃ emissions and bidirectional air–surface exchange is critical for reducing uncertainties in the GEOS-Chem model, which may in turn afford better top-down constraints on NH₃ source distributions and seasonal variations. In this paper, we apply a new diurnal distribution pattern to NH₃ livestock emissions in GEOS-Chem, which is developed based on observations of emissions in the Concentrated Animal Feeding Operation (CAFO) dominated areas in North Carolina (Zhu et al., 2015). We then implement bidirectional exchange of NH₃ in a global chemical transport model – GEOS-Chem – following Pleim et al. (2013) and compare the model to in situ observations. As a first step towards including bidirectional exchange in NH₃ inverse modeling, we also develop the adjoint of bidirectional exchange in GEOS-Chem; this also provides a useful method for quantifying the sensitivities of GEOS-Chem simulations with respect to important parameters in the bidirectional model, such as soil pH and fertilizer (only mineral fertilizer is considered in NH₃ bidirectional exchange) application rate, which are themselves uncertain.

Section 2 describes the model we use in this study. Section 3 introduces the in situ observation networks we use for evaluation. The impacts of implementing the new diurnal variation pattern of NH₃ emissions are presented in Sect. 4. The details of developing bidirectional exchange and its adjoint in GEOS-Chem are described in Sect. 5, followed by the evaluations and adjoint sensitivity analysis in Sect. 6. We present our conclusions in Sect. 7.

2 Methods

2.1 GEOS-Chem

GEOS-Chem is a chemical transport model driven with assimilated meteorology from the Goddard Earth Observing System (GEOS) of the NASA Global Modeling and Assimilation Office (Bey et al., 2001). We use the nested grid of the model (horizontal resolution 1/2° × 2/3° (~ 50 km × 67 km) over the USA and 2° × 2.5° (~ 200 km × 250 km) horizontal resolution for the rest of the world). The year 2008 is simulated with a spin-up period of 3 months. The tropospheric oxidant chemistry simulation in GEOS-Chem includes a detailed ozone–NO_x–hydrocarbon–aerosol chemical mechanism (Bey et al., 2001) coupled with a sulfate–nitrate–ammonia aerosol thermodynamics module described in Park et al. (2004). The wet deposition scheme of soluble aerosols and gases is described in Liu et al. (2001). The dry deposition of aerosols and gases scheme is based on a resistance-in-series model (Wesely, 1989), updated here to include bidirectional exchange (see Sect. 5).

Global anthropogenic and natural sources of NH₃ are from the GEIA inventory 1990 (Bouwman et al., 1997). The anthropogenic emissions are updated by the following regional

inventories: the 2005 US EPA National Emissions Inventory (NEI) for the USA, the Criteria Air Contaminants (CAC) inventory for Canada (van Donkelaar et al., 2008), the inventory of Streets et al. (2006) for Asia, and the co-operative program for monitoring and evaluation of the long-range transmission of air pollutants in Europe (European Monitoring and Evaluation Program, EMEP) inventory for Europe (Vestreng and Klein, 2002). Monthly biomass burning emissions are from van der Werf et al. (2010), and biofuel emissions are from Yevich and Logan (2003). The anthropogenic emissions inventories described here are only used for base case nested grid model runs over the USA. Variants will be explained in the following sections. Table 1 is a summary of various emissions inventories used in different sections.

2.2 GEOS-Chem adjoint model

An adjoint model is an efficient tool for investigating the sensitivity of model estimates with respect to all model parameters simultaneously. This approach has been applied in recent decades in chemical transport models for source analysis of atmospheric tracers (Fisher and Lary, 1995; Elbern et al., 1997) and for constraining emissions of tropospheric chemical species (Elbern et al., 2000). Adjoint models have also been used in air quality model sensitivity studies (e.g., Martien and Harley, 2006). The adjoint of GEOS-Chem is fully described and validated in Henze et al. (2007). It has been used for data assimilation using in situ observations (e.g., Henze et al., 2009; Paulot et al., 2014) and remote sensing observations (e.g., Kopacz et al., 2010; Zhu et al., 2013; Xu et al., 2013). In this paper, we develop the adjoint of bidirectional exchange and we use this adjoint model to investigate the sensitivity of modeled NH₃ with respect to soil pH and fertilizer application rate.

3 Observations

Surface measurements

We use surface observations of NH₃ and wet deposited NH₄⁺ from several networks to evaluate model estimates.

The SouthEastern Aerosol Research and Characterization (SEARCH) network contains monitoring stations throughout the southeastern USA. The SEARCH network provides different sampling frequencies, such as daily, 3-day, 6-day, 1 min, 5 min, and hourly, at different sites. Three of the monitoring stations (Oak Grove, MS, Jefferson Street, GA, and Yorkville, GA) provide 5 min long surface NH₃ observations. In order to see the diurnal variations, we convert the 5 min long observations to be hourly average NH₃ concentration for each of these three sites in July 2008. We then average the hourly observations of these three sites to compare with the modeled results of corresponding sites.

The Ammonia Monitoring Network (AMoN) of the National Atmospheric Deposition Program (NADP) contains

21 sites across the USA with 2-week-long sample accumulation (Puchalski et al., 2011). We average the 2-week-long observations from November 2007 through June 2010 to monthly NH₃ concentrations. The Interagency Monitoring of Protected Visual Environments (IMPROVE) network (Malm et al., 2004) consists of more than 200 sites in the continental USA which collect PM_{2.5} particles over 24 h every third day. We use monthly average sulfate and nitrate aerosols concentrations.

We use wet NH₄⁺ deposition observations from several monitoring networks around the world. The NADP National Trends Network (NTN) (<http://nadp.sws.uiuc.edu/NTN>) contains more than 200 sites in the USA which are predominately located in rural areas. It provides wet deposition observations of ammonium with week-long sample accumulation. The Canadian Air and Precipitation Monitoring Network (CAPMoN) (<http://www.on.ec.gc.ca/natchem>) contains about 26 sites which are predominately located in central and eastern Canada with 24 h integrated sample times. The EMEP network (<http://www.nilu.no/projects/cce/emepdata.html>) contains about 70 sites which are predominately located away from local emission sources. It has daily, weekly, and biweekly observations of ammonium available in different sites. The Acid Deposition Monitoring Network in eastern Asia (EANET) (<http://www.eanet.asia/product>) contains 54 sites (21 urban, 13 rural, and 20 remote sites) with monthly observations of wet deposition of ammonium. We only use nonurban sites (~30) of EANET to avoid large local emission sources influences. We convert the daily/weekly/biweekly observations to monthly average NH₄⁺ concentration in 2008.

4 Diurnal variability of ammonia livestock emission

4.1 Development of new diurnal distribution scheme

Simulated NH₃ surface concentrations in GEOS-Chem are significantly overestimated at nighttime compared to hourly observations from the SEARCH network (Zhu et al., 2013). The standard NH₃ emissions in GEOS-Chem are evenly distributed throughout the 24 h of each day of the month, as indicated by the blue line in Fig. 1. That the simulated NH₃ emissions do not have any diurnal variation is a likely explanation for this discrepancy with hourly observation. Thus, a new diurnal distribution scheme for NH₃ livestock emissions has been developed in CMAQ (Zhu et al., 2015). Here we implement this algorithm in GEOS-Chem. The hourly NH₃ livestock emission, $E_h(t)$, is calculated from the monthly total emission, E_m , as

$$E_h(t) = E_m N_{\text{met}}(t), \quad (1)$$

where $N_{\text{met}}(t)$ is the hourly fraction of the NH₃ livestock emission during the month. This depends on the aerodynamic

Table 1. A summary of various emissions inventories used in different sections.

Section	Region	Horizontal resolution	Model version	Anthropogenic emissions inventory	Gross emissions in region (Tg)		
					April	July	October
4.2	USA ^a	1/2° × 2/3°	Static and dynamic	NEI 2005 ^b	0.200	0.407	0.223
4.3	Global	2° × 2.5°	Static and dynamic	MASAGE_NH3 ^c	6.79	6.59	5.01
6.1.1, 6.1.2	USA	1/2° × 2/3°	BASE ^d	NEI 2005	0.200	0.407	0.223
			BIDI ^d	NEI 2005 livestock + upward BIDI flux ^e	0.153	0.428	0.192
6.1.3	USA	2° × 2.5°	BASE	Optimized emissions inventories ^f	1.04	1.11	1.27
			BIDI		1.12	1.21	1.40
6.2, 6.3, 6.4	Global	2° × 2.5°	BASE	MASAGE_NH3	6.79	6.59	5.01
			BIDI		5.62	6.30	4.73

^a Continental USA. ^b NEI 2005 does not distinguish the livestock emissions sector. Thus, the livestock fractions calculated from NEI 2008 are used in the dynamic case.

^c MASAGE_NH3 contains livestock and fertilizer sectors. ^d All BASE and BIDI cases include the new dynamic scheme. ^e In all BIDI cases, fertilizer emissions in BASE case will be replaced by the upward BIDI flux. ^f Optimized emissions inventories from Zhu et al. (2013).

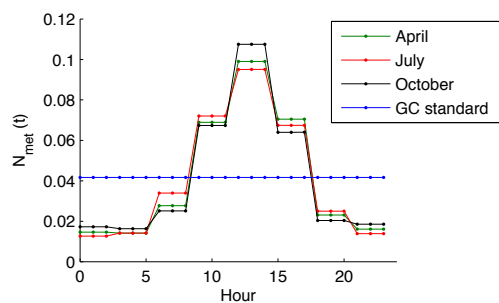


Figure 1. Monthly averaged diurnal variation fractions of livestock emissions of year 2008 over the USA. The blue line is the standard GEOS-Chem. Dark green, red, and black lines are the newly developed diurnal pattern of NH₃ livestock emissions in April, July, and October, respectively.

resistance, R_a [$s^{-1} m$], and surface temperature, T [K]:

$$N_{\text{met}}(t) = \frac{H(t)/R_a(t)}{\sum_{t=1}^n (H(t)/R_a(t))}, \quad (2)$$

where n is the number of hours in a month, t is the time during the month, from 1 to n , and $H(t)$ is the Henry's equilibrium, calculated following Nemitz et al. (2000):

$$H(t) = \frac{161\,500}{T} e^{-10\,380/T}. \quad (3)$$

More details of the development of this diurnal variability scheme can be found in Zhu et al. (2015).

4.2 Evaluation with in situ NH₃ observations

We replace the standard GEOS-Chem livestock emissions, which are evenly distributed for each hour of the day (static), with this new diurnal variability of livestock emissions that peaks in the middle of the day (dynamic) (Fig. 1). This also introduces daily variability of livestock emissions into the

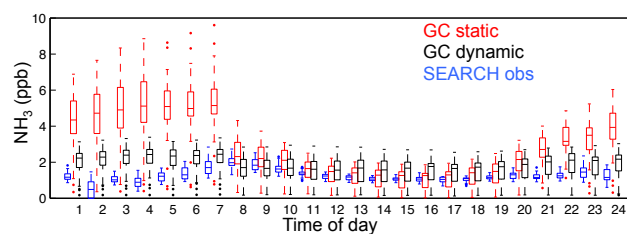


Figure 2. Diurnal variation of NH₃ surface concentrations from SEARCH observations (blue) and GEOS-Chem model with (black) and without (red) dynamic emissions scheme in July 2008.

simulation, which is not considered in the standard GEOS-Chem model. As the standard GEOS-Chem anthropogenic emissions do not distinguish the livestock emissions sector (described in Sect. 2.1), we calculate the absolute NH₃ livestock emissions based on the fraction of livestock emissions in anthropogenic emissions in the 2008 NEI.

Significant improvements are found when we compare surface NH₃ concentrations to SEARCH observations after implementing the dynamic diurnal emissions (see Fig. 2). The dynamic case (black) decreases the surface NH₃ concentration relative to the static case (red) by several ppb at night and increases concentrations slightly (up to 1 ppb) in the day. This reduces the model mean bias by up to 2.9 ppb at night.

4.3 Global distribution

To apply the dynamic emissions scheme globally, we implement a new global NH₃ anthropogenic emissions inventory Magnitude And Seasonality of AGricultural Emissions model (MASAGE_NH₃; Paulot et al., 2014), which contains sector-specific emissions for different agriculture sources, such as livestock emissions (the standard GEOS-Chem NH₃ emissions do not clearly distinguish this sector). Comparisons between the emissions of MASAGE_NH₃ and GEOS-

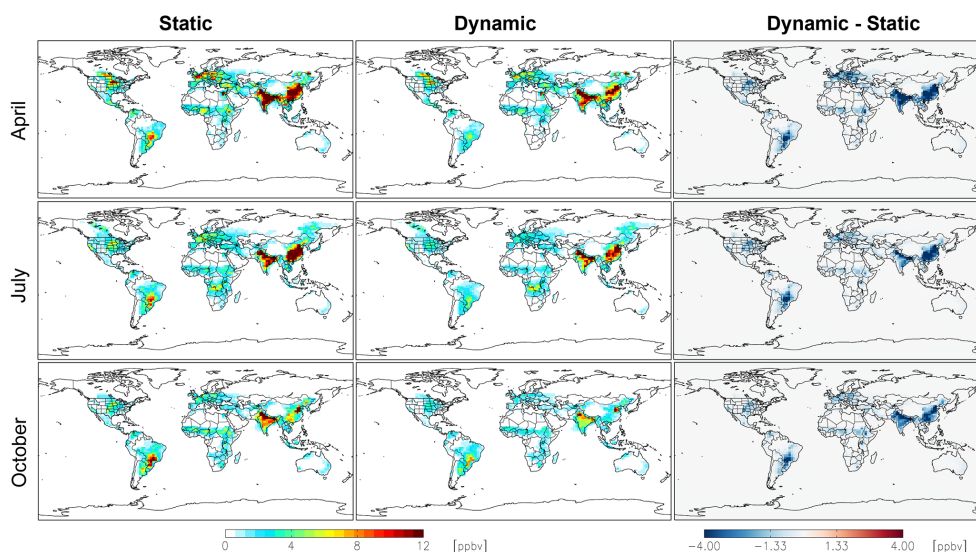


Figure 3. Spatial distribution of GEOS-Chem simulated NH_3 concentration at surface level in static cases, dynamic cases, and their differences. Monthly averages are shown for April, July, and October of 2008.

Chem standard inventories are in Paulot et al. (2014). Figure 3 shows the global distribution of surface NH_3 concentrations from the GEOS-Chem static and dynamic cases in April, July, and October of 2008. The third column shows the difference between the dynamic and the static cases. In general, the dynamic case decreases the monthly NH_3 surface concentration throughout the world with significant changes in southeast China and India in all 3 months, which can be up to 17.1 ppb in China in October and 12.1 ppb in India in April. There are also large decreases in the eastern USA (up to 3.3 ppb) and southeastern South America.

The modeled representative volume mixing ratio (RVMR) (Shephard et al., 2011) underestimates the observed RVMR from TES in the USA and most places of the globe (Shephard et al., 2011; Zhu et al., 2013). In this study, we also compare the modeled RVMR from static and dynamic cases to the TES RVMR. We calculate modeled RVMR at the same time and locations of TES retrievals during 2006 through 2009. We average the RVMRs at the $2^\circ \times 2.5^\circ$ grid resolution for each month (April, July, and October). The static RVMR underestimates the TES RVMR throughout the globe in all 3 months except in India and southeastern China in April. With the new diurnal variability scheme (dynamic case), the modeled RVMR increases in many places (e.g., eastern China, northern India, South America) and decreases in the mid-USA and northern Europe. The differences between the dynamic and static RVMR are from -1.5 to 1.6 ppb. These changes generally reduce differences between modeled and observed RVMR, while the differences are enhanced in a few locations, such as northern India in April. However, the magnitude of these changes is small compared to the differences (from -11.4 to 3 ppb) between the static RVMR and TES RVMR. We are able to detect more obvious changes between

the static and dynamic cases when focusing on a livestock source region (California) and a hotter day, during which the dynamic RVMR increases 3.4 ppb (Zhu et al., 2015). Stronger constraints on diurnal variability would be evident from potential future geostationary measurements (Zhu et al., 2015).

High biases of surface nitrate aerosol concentrations in GEOS-Chem are found in the USA (e.g., Heald et al., 2012; Walker et al., 2012). Here we consider the impact of dynamic NH_3 livestock emissions on surface nitrate concentration in the USA as well as globally. Figure 4 presents the global distribution of surface nitrate concentration from the GEOS-Chem static and dynamic cases in April, July, and October of 2008. The dynamic case decreases the nitrate concentration significantly in eastern China in all 3 months, which can be as large as $7 \mu\text{g m}^{-3}$ in October. There are also large decreases in the eastern USA which can be up to $2.7 \mu\text{g m}^{-3}$ in July. In October, there are large decreases in the dynamic case in comparison to static case in northern India (up to $3.9 \mu\text{g m}^{-3}$) and Europe (up to $2.4 \mu\text{g m}^{-3}$ in Poland).

Investigating the impacts of dynamic NH_3 livestock emissions on nitrogen deposition is also of interest. In Fig. 5, we show the global distribution of total nitrogen deposition (wet deposition of NH_3 , ammonium, HNO_3 and nitrate and dry deposition of NH_3 , ammonium, NO_2 , PAN, N_2O_5 , HNO_3 , and nitrate) from GEOS-Chem static and dynamic cases in April, July, and October of 2008. The dynamic case decreases nitrogen deposition in most places in the world, yet increases it in several locations. The largest decrease of nitrogen deposition occurs in northern India in April by up to $3.6 \text{ kg N ha}^{-1} \text{ month}^{-1}$. The total amount of nitrogen deposition in India decreases by 8.6% in April. Decreases in nitrogen deposition in the dynamic case occur in southeastern

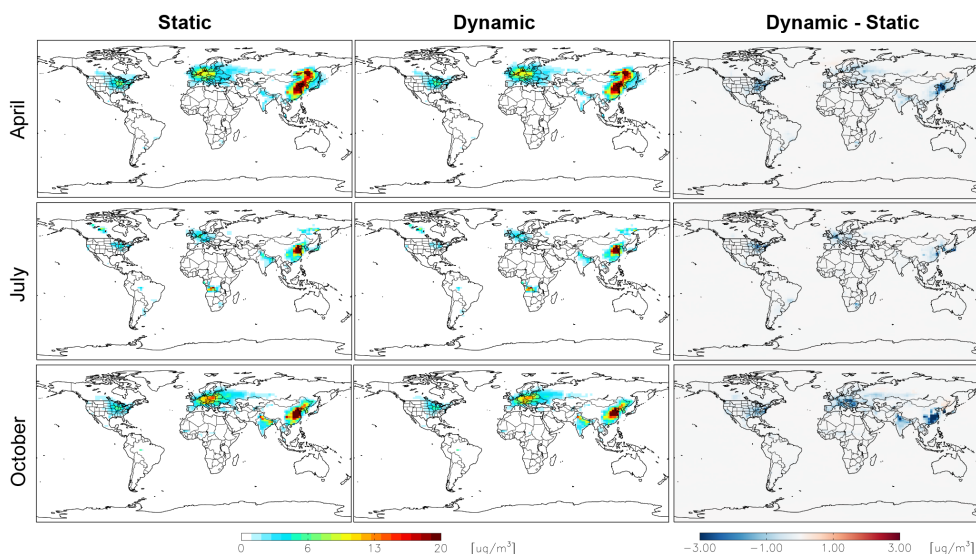


Figure 4. Spatial distribution of GEOS-Chem simulated nitrate concentration at surface level in static cases, dynamic cases, and their differences. Monthly averages are shown for April, July, and October of 2008.

China in all 3 months, with the total amount of nitrogen deposition in China decreasing by 4.7 % in April, 2.8 % in July, and 3.1 % in October. The new diurnal variability scheme has more NH₃ from livestock emissions emitted in the daytime, when the boundary layer is thicker than nighttime. Typically, this lowers deposition largely at night. However, it may also be conducive to more export of NH₃ in the atmosphere during the day. Thus, slight increases of nitrogen in the dynamic cases occur downwind of regions with large NH₃ sources in the base cases, such as increases in northeastern China owing to enhanced NH₃ export from eastern China.

5 Bidirectional exchange of NH₃

5.1 Bidirectional flux calculation

The dry deposition scheme in the standard GEOS-Chem model is based on the resistance in series formulation of Wesely (1989), which only considers the unidirectional flux of NH₃ from the air to the surface. However, the air–surface exchange is known to actually be bidirectional. In this paper, we update the dry deposition of NH₃ to combine NH₃ dry deposition from the atmosphere and emission from vegetation. A simplified schematic of the updated air–surface exchange process of NH₃ is shown in Fig. 6. More details of this bidirectional scheme can be found in Cooter et al. (2010) and Pleim et al. (2013). The total air–surface exchange flux, F_t , is calculated as a function of the gradient between the ambient NH₃ concentration in the first (surface) layer of the model and the canopy compensation point (Bash et al., 2013; Pleim et al., 2013):

$$F_t = \frac{C_c - C_a}{R_a + 0.5R_{inc}}, \quad (4)$$

where C_a is the ambient NH₃ concentration of the first atmospheric layer of the model, C_c is the canopy compensation point (which is set at one half of the in-canopy resistance, since NH₃ can come from either air or soil to the canopy, thus, splitting R_{inc} symmetrically is appropriate), R_a is the aerodynamic resistance, and R_{inc} is the in-canopy aerodynamic resistance. $C_a > C_c$ will result in deposition from air to surface, and $C_a < C_c$ will result in emission from surface to air. C_c is calculated as (Bash et al., 2013)

$$C_c = \quad (5)$$

$$\frac{\frac{C_a}{R_a + 0.5R_{inc}} + \frac{C_{st}}{R_b + R_{st}} + \frac{C_g}{0.5R_{inc} + R_{bg} + R_{soil}}}{(R_a + 0.5R_{inc})^{-1} + (R_b + R_{st})^{-1} + (R_b + R_w)^{-1} + (0.5R_{inc} + R_{bg} + R_{soil})^{-1}},$$

where R_b , R_{bg} , R_{st} , R_{soil} , and R_w are the resistances at the quasi-laminar boundary layer of leaf surface, the quasi-laminar boundary layer of ground surface, the leaf stomatal, soil, and cuticle, respectively. R_a , R_b , R_{bg} , R_{st} , and R_w are already defined and used in the standard GEOS-Chem deposition scheme. Here we define and calculate R_{soil} and R_{inc} following Pleim et al. (2013). C_{st} and C_g are the NH₃ concentrations in the leaf stomata and soil pores, respectively. They are calculated as functions of temperature and NH₃ emission potential ($\Gamma_{st,g}$, dimensionless) in the leaf stomata and soil (Nemitz et al., 2000).

$$\Gamma = \frac{[\text{NH}_4^+]}{[\text{H}^+]} \quad (6)$$

Γ_{st} is calculated as a function of land cover type, and the values of different land cover types are based on Zhang et al.

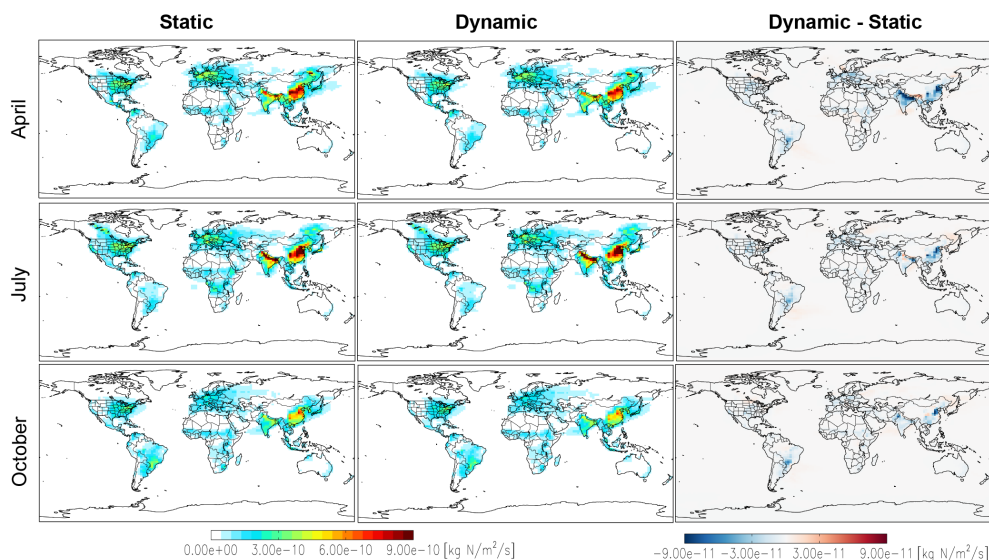


Figure 5. Spatial distribution of GEOS-Chem simulated total N deposition in static cases, dynamic cases, and their differences. Monthly averages are shown for April, July, and October of 2008.

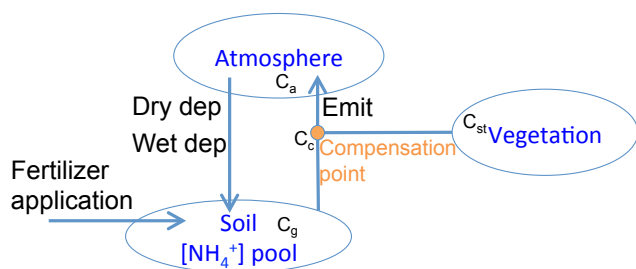


Figure 6. Simplified schematic of NH₃ bidirectional exchange model. C_a , C_g , and C_{st} are the NH₃ concentrations in the atmosphere, soil, and stomata, respectively. C_c is the NH₃ concentration at the canopy compensation point.

(2010). Γ_g is calculated as a function of soil pH and NH₄⁺ concentration in the soil, [NH₄⁺]_{soil}. Soil pH data are taken from ISRIC – World Soil Information with a 0.5° × 0.5° global resolution (<http://www.isric.org/data/data-download>). We model the [NH₄⁺]_{soil} as an ammonium pool in the soil, which is a function of fertilizer application rate, deposition, nitrification, soil moisture, and emission in bidirectional exchange. The calculation of [NH₄⁺]_{soil} is described in the next section.

To compare the deposition (downward) flux and emission (upward) flux of the bidirectional case to the base case, we define diagnostic variables for gross deposition flux F_{dep} and emission flux F_{emis} as follows (Bash et al., 2013),

$$F_{\text{dep}} = \frac{C_c - C_a}{R_a + 0.5R_{\text{inc}}} \Big|_{C_{st}=0, C_g=0}, \quad (7)$$

$$F_{\text{emis}} = \frac{C_c}{R_a + 0.5R_{\text{inc}}} \Big|_{C_a=0}, \quad (8)$$

where F_{dep} is calculated under the assumption that there is no NH₃ emission potential from the soil and canopy, and F_{emis} is calculated under the assumption that there is no NH₃ in the atmosphere. Thus, $F_{\text{dep}} + F_{\text{emis}} = F_t$.

5.2 Soil ammonium pool

Here we introduce a NH₄⁺ pool to track the NH₃ and NH₄⁺ in the atmosphere and in the soil. The inputs to the ammonium pool in the soil are NH_x (NH₃ and NH₄⁺) deposition from the atmosphere, NH₃ emission from the soil, and N fertilizer application rate. The annual N fertilizer application rates are from Potter et al. (2010), which have chemical fertilizer (global total 70 Tg N yr⁻¹) with a 0.5° × 0.5° resolution for the year 2000. We assume that all forms of N fertilizers will convert to NH₄⁺ rapidly after fertilizer application. This data set is also used to develop the global soil nitric oxide emissions in GEOS-Chem in Hudman et al. (2012). We use the same treatment of annual total fertilization as Hudman et al. (2012) to derive daily fertilizer application rates by applying 75 % of the annual total fertilization amount around the first day of the growing season (green-up day), distributed with a Gaussian distribution 1 month after. The other 25 % is evenly distributed over the remaining time before the end of the growing season (brown-down day). The determination of green-up and brown-down days is based on the growing season dates derived from the MODIS Land Cover Dynamics product (MCD 12Q2) using the MODIS enhanced vegetation index (Hudman et al., 2012).

Using the fertilizer inputs described above, in addition to inputs from deposition and outputs from emission, the time-dependent soil NH₄⁺ pool [mol L⁻¹] is calculated as

$$[\text{NH}_4^+]_{\text{soil}} = \frac{[\text{NH}_x]_{\text{dep}}}{d_s \theta N_A} + \frac{[\text{N}]_{\text{fert}}}{d_s \theta M_N} - \frac{[\text{NH}_3]_{\text{bidi emit}}}{d_s \theta N_A}, \quad (9)$$

where $[\text{NH}_x]_{\text{dep}}$ [molec cm⁻²] is deposition from wet and dry deposition of NH₃ and NH₄⁺, $[\text{N}]_{\text{fert}}$ [N g m⁻²] is the NH₄⁺ from fertilizer, $[\text{NH}_3]_{\text{bidi emit}}$ [molec cm⁻²] is the gross NH₄⁺ emitting from the soil due to bidirectional exchange, M_N is the molar mass of nitrogen, d_s is the depth of the soil layer, taken to be 0.02 m, θ is the soil wetness [m³ m⁻³], and N_A is Avogadro's number. We then solve the mass balance equation for $[\text{NH}_x]_{\text{dep}}$ and $[\text{N}]_{\text{fert}}$:

$$\frac{d[\text{NH}_x]_{\text{dep}}}{dt} = S_{\text{dep}} - \frac{[\text{NH}_x]_{\text{dep}}}{\tau} - L_{\text{dep}}, \quad (10)$$

$$\frac{d[\text{N}]_{\text{fert}}}{dt} = S_{\text{fert}} - \frac{[\text{N}]_{\text{fert}}}{\tau}, \quad (11)$$

where τ is the decay time owing to nitrification rate of NH₄⁺ in soil. We assume τ is 15 days, since almost all NH₄⁺ will convert to NO₃⁻ within that timespan (Matson et al., 1998). S_{dep} is the deposition rate, S_{fert} is the fertilizer application rate, and L_{dep} is the deposition loss rate. We use the same assumption as Hudman et al. (2012) that only 60 % of this deposited NH_x will enter the soil, while the rest of the NH_x deposition will runoff into waterways. Here we do not consider the production of NH₄⁺ from NO₃⁻ in the nitrogen cycle from mineralization nor immobilization. The timescale of these processes can be years, which is much larger than the timescale of the NH₄⁺ simulations considered here; Cooter et al. (2010) also found these processes were not needed to accurately simulate NH₃ over managed lands on similar timescales.

5.3 Adjoint of bidirectional exchange

To investigate the sensitivity of modeled NH₃ concentrations to the parameters in the bidirectional exchange model, and to facilitate future inverse modeling, we develop the adjoint of our updated NH₃ flux scheme. Here we consider two key parameters, soil pH and fertilizer application rate, since their values are highly approximate.

The adjoint sensitivity is defined as

$$\lambda_\sigma = \frac{\partial J(\text{NH}_3)}{\partial \sigma}, \quad (12)$$

where $J(\text{NH}_3)$ is the total mass of ammonia at surface level in each grid box during 1 week. The unit of $J(\text{NH}_3)$ is kg box⁻¹. σ in this study is defined as the soil pH scaling factor (σ_{pH}) or fertilizer application rate scaling factor ($\sigma_{\text{fert_rate}}$). σ_{pH} is defined as $\frac{\text{pH}}{\text{pH}^0}$ and $\sigma_{\text{fert_rate}}$ is defined as

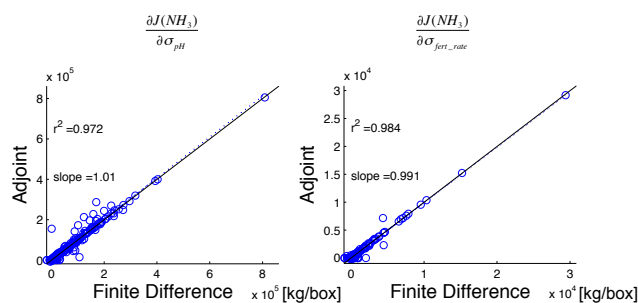


Figure 7. The adjoint sensitivity of NH₃ surface level concentration with respect to soil pH (left) and fertilizer application rate (right) compared to finite difference gradients. The cost function is evaluated once at the end of a 1-week simulation which excludes horizontal transport.

$\frac{\text{fert_rate}}{\text{fert_rate}^0}$, pH^0 and fert_rate^0 are the initial estimate of soil pH from ISRIC and fertilizer application rates from Potter et al. (2010). λ_σ is the sensitivity of $J(\text{NH}_3)$ with respect to the bidirectional exchange model parameters σ .

5.4 Validating the adjoint of bidirectional exchange

We validate the accuracy of the adjoint model by comparing the sensitivity of NH₃ surface concentrations with respect to soil pH and fertilizer application rate calculated using the adjoint model with sensitivities calculated using the finite differences method. In order to make such comparisons efficiently throughout the model domain, horizontal transport is turned off for these tests (e.g., Henze et al., 2007). Figure 7 shows the comparison of sensitivities calculated by adjoint and finite difference. The slope of a linear regression and square of correlation coefficient, R^2 , are both close to unity, demonstrating the accuracy of adjoint of the bidirectional model.

6 Results and discussion

For the US region, we use nested horizontal resolution (1/2° × 2/3°) simulations with the standard set of GEOS-Chem emission inventories. For the global simulation, we introduce a new bottom-up emission inventory for NH₃ agriculture sources, MASAGE_NH3 (Paulot et al., 2014). The full description of the differences between the GEOS-Chem standard NH₃ emission inventories and MASAGE_NH3 is in Paulot et al. (2014). We perform global simulation at a horizontal resolution of 2° × 2.5°. All simulations include the dynamic treatment of the diurnal variability of livestock emissions described in Sect. 4.

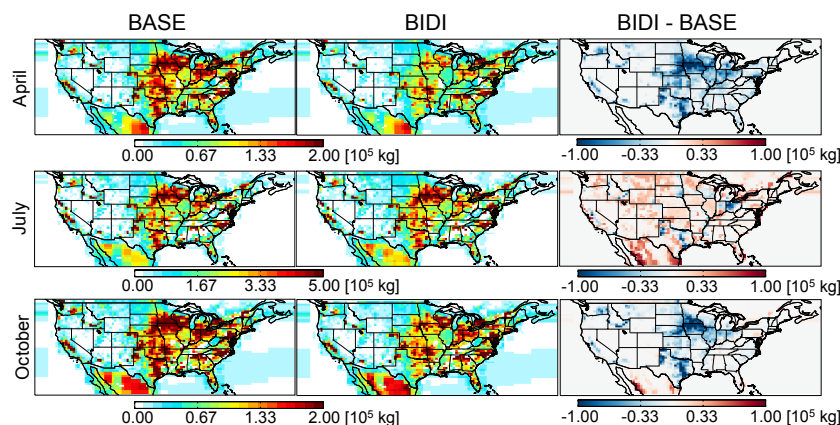


Figure 8. Spatial distribution of ammonia total emissions from GEOS-Chem with (BIDI) and without (BASE) bidirectional exchange and their differences in April, July, and October of 2008. The total emissions in the BIDI case are the sum of upward fluxes from soil and vegetation from the bidirectional exchange and emissions from all other sources except fertilizers.

6.1 USA

We run the GEOS-Chem model for April, July, and October of 2008 with the updated diurnal variation of NH_3 livestock emissions and the bidirectional exchange mechanism. Figure 8 shows the NH_3 total gross emissions from GEOS-Chem with (BIDI) and without (BASE) the bidirectional air-surface exchange. The total gross emissions of BIDI case are the sum of primary emissions and upward fluxes from soil and vegetation. Bidirectional exchange generally increases gross emissions in most parts of the USA in July (up to $0.43 \text{ Gg month}^{-1}$) and decreases gross emissions throughout the USA in October (up to $0.29 \text{ Gg month}^{-1}$). Significant decreases occur in the Great Plains region in both April and October with a magnitude of up to $0.23 \text{ Gg month}^{-1}$ in April and $0.29 \text{ Gg month}^{-1}$ in October. Bidirectional exchange does not much alter the total modeled emissions in the USA in July (increase by 5.2 %) and October (decrease by 13.9 %) but does lead to a decrease of 23.5 % in April. With the ammonium soil pool, the model can preserve ammonia/ammonium in the soil rather than emitting it directly after fertilizer application. This is the main reason that gross emissions decrease in the Great Plains in April and October. In July, there is not as much fertilizer applied as in April. However, the bidirectional exchange between the air and surface can induce NH_3 to be re-emitted from the ammonium soil pool which reserve ammonium from previous deposition and fertilizer application.

The spatial distributions of surface NH_3 concentrations in GEOS-Chem are shown in Fig. 9. In general, bidirectional exchange decreases monthly NH_3 surface concentrations in April (up to 1.8 ppb) and October (up to 2.1 ppb) and increases it in July (up to 2.8 ppb) throughout the USA. There are peak decreases in NH_3 surface concentrations in the Great Plains in both April and October and increases in California in July. These changes of surface NH_3 concentra-

tion are consistent with the pattern of changes to NH_3 emissions in Fig. 8.

6.1.1 Evaluation with NH_3

We evaluate the GEOS-Chem simulation with bidirectional exchange by comparing the model values to in situ observations from AMoN. Figure 10 shows the comparison of GEOS-Chem surface NH_3 concentrations in the BASE and BIDI cases with AMoN observations. Bidirectional exchange decreases the normalized mean bias (NMB) from -0.227 to -0.165 in July and increases the NMB from -0.701 and -0.197 to -0.829 and 0.283 in April and October, respectively. The root mean square error (RMSE) decreases by 18.3 % in July and increases by 16.7 % in April and 19.2 % in October. R^2 values increase by 20.6 % in July and decrease by 37.6 % in April and 49.1 % in October. The slope slightly increases by 0.5 % in July and decreases by 53.5 and 37.5 % in April and October, respectively. The changes in slopes can also be seen in Fig. 9 as bidirectional exchange decreases the NH_3 monthly average concentration at AMoN sites in April and October while it increases the NH_3 monthly average concentrations in July. Modeled surface NH_3 concentrations are significantly lower than the AMoN observations in April and October by a factor of 2–5, which is not unreasonable given likely underestimation in primary emissions (Zhu et al., 2013; Nowak et al., 2012; Schiferl et al., 2014). Such large underestimation is not corrected by applying the NH_3 bidirectional exchange to the model. Other improvements in the model besides bidirectional exchange, such as updating primary NH_3 emissions, are also required for better estimating NH_3 surface concentrations.

6.1.2 Evaluation with aerosol nitrate

We also compare the simulated nitrate aerosol concentrations to the aerosol observations from IMPROVE. Figure 11

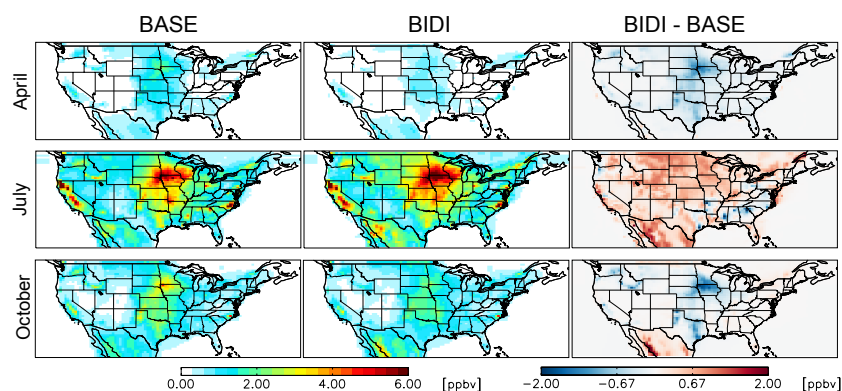


Figure 9. Spatial distribution of ammonia concentration at surface level of GEOS-Chem with (BIDI) and without (BASE) bidirectional exchange and their differences in April, July, and October of 2008.

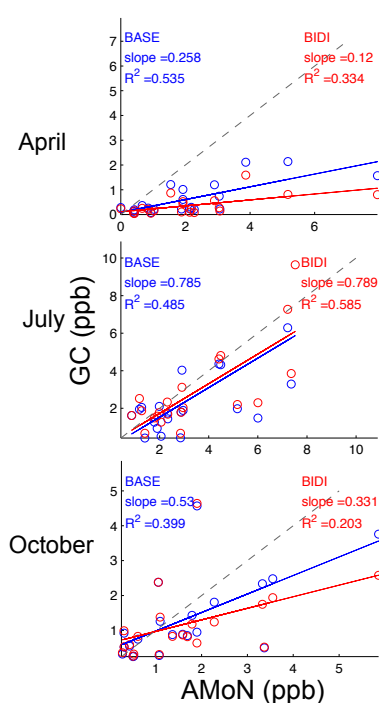


Figure 10. Comparison of GEOS-Chem simulated NH_3 concentration at surface level in BASE and BIDI cases with AMoN observations in April, July, and October of 2008. R^2 is the square of the correlation coefficient. Solid lines are regressions. Gray dashed lines are 1 : 1.

shows the simulated monthly average nitrate aerosol surface concentration from the GEOS-Chem BASE and BIDI cases in comparison to IMPROVE observations in 2008. GEOS-Chem overestimates nitrate in the BASE case in all 3 months. The overestimates in BASE cases can be 5 times larger in October. Bidirectional exchange generally decreases the nitrate concentrations in April, which makes the slope of the regression line decrease by 45.4%. However there are still large overestimates (\sim a factor of 2 on average) in the North-

eastern USA and large underestimates (up to $1.7 \mu\text{g m}^{-3}$) in Southern California in the BIDI case in April. Bidirectional exchange slightly increases (less than $0.5 \mu\text{g m}^{-3}$) nitrate in July and decreases (less than $0.4 \mu\text{g m}^{-3}$) nitrate in October, which does not significantly impact the comparison of modeled nitrate with IMPROVE observations.

Overestimation of nitrate in GEOS-Chem is a long recognized problem (Park et al., 2004; Liao et al., 2007; Henze et al., 2009; Heald et al., 2012; Walker et al., 2012; Zhu et al., 2013). Heald et al. (2012) recommend that reducing the nitric acid to 75 % would bring the magnitude of nitrate aerosol concentration into agreement with the IMPROVE observations. In our study, based on the comparison of BASE modeled nitrate concentration and IMPROVE observation, we perform sensitivity studies by reducing the nitric acid to 50 % in July and to 20 % in October at each time step in the GEOS-Chem model for both BASE and BIDI cases. Modeled nitrate concentrations reduce dramatically with this adjustment in July and October, but overestimates still exist in many places in the eastern USA. We also compare the modeled NH_3 surface concentrations in the sensitivity simulations with adjusted nitric acid concentrations to the AMoN observations, since reducing the nitric acid in the model may cause NH_3 to partition more to the gas phase, which could bring modeled NH_3 concentrations into better agreement with AMoN observations. However, no significant impacts are found in NH_3 concentrations at AMoN site locations with these nitric acid adjustments, consistent with earlier assessments that the model's nitrate formation is NH_3 limited throughout much of the USA (Park et al., 2004). Overall, overestimation of model nitrate by a factor of 3 to 5 appears to be a model deficiency beyond the issue of NH_3 bidirectional exchange.

6.1.3 Comparison to inverse modeling

Inverse modeling estimates of unidirectional NH_3 emissions using TES observations lead to overestimates of ammonia concentration in comparison to surface observations from

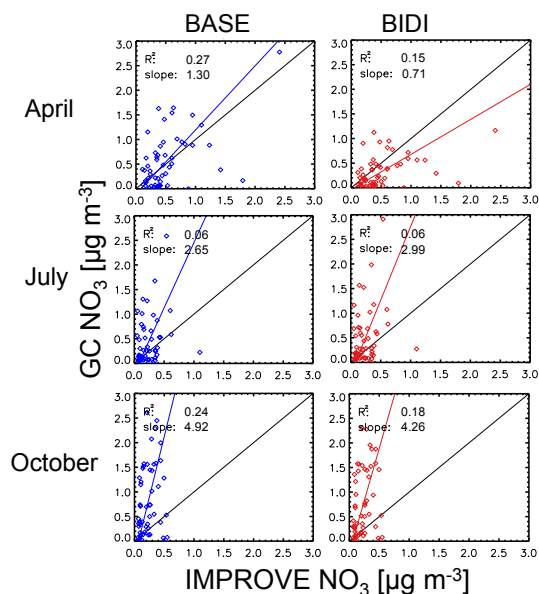


Figure 11. Comparison of GEOS-Chem simulated nitrate aerosol concentration at surface level in BASE and BIDI cases with IMPROVE observations in April, July, and October of 2008. R is the correlation coefficient.

AMoN in July (Zhu et al., 2013), and emissions estimates in July are much higher than other top-down or bottom-up studies (Paulot et al., 2014). It is thus of interest to evaluate whether bidirectional exchange of NH_3 would reduce this high bias. Although repeating the inverse modeling with TES NH_3 observations and bidirectional exchange is beyond the scope of this work, we can use the optimized emissions from Zhu et al. (2013) as the basis upon which bidirectional exchange is applied. Figure 12 shows the modeled NH_3 monthly average surface concentrations in comparison to the AMoN observations. The left column of Fig. 12 is from the optimized NH_3 estimates from Zhu et al. (2013). In the right column, the modeled NH_3 monthly average concentrations are from GEOS-Chem with NH_3 bidirectional exchange using the optimized emissions from Zhu et al. (2013). The model with bidirectional exchange decreases the high bias in July: the NMB decreases by 80.4 % and the RMSE decreases by 56.7 %. The R^2 value increases by 43.3 %. However, the model with bidirectional exchange now underestimates the NH_3 monthly average concentrations in April and October. The RMSE increases by 4.1 % in April and 28.8 % in October. The impacts of NH_3 concentration with respect to emissions in the model with bidirectional exchange are nonlinear. Using the optimized NH_3 emissions inventories from the TES NH_3 assimilation with the BASE model does not guarantee a better estimation of NH_3 surface concentrations with the BIDI model. Therefore, full coupling of inverse modeling with TES NH_3 observations and bidirectional exchange is necessary. Also, investigating the sensitivities of bidirectional model results to the NH_3 emissions, as well as other

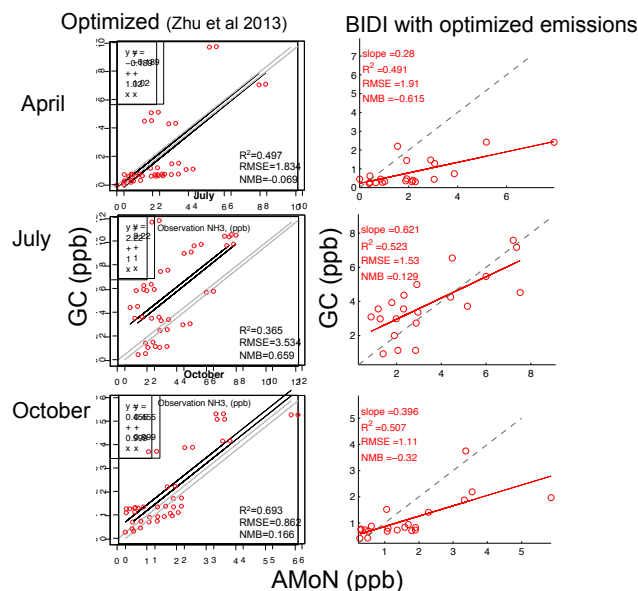


Figure 12. Left column: comparison of GEOS-Chem optimized NH_3 concentration at surface level from Zhu et al. (2013) with AMoN observations. Right column: comparison of GEOS-Chem simulated NH_3 concentration at surface level in BIDI case using optimized NH_3 emissions from Zhu et al. (2013) with AMoN observations. R^2 is the square of the correlation coefficient. Gray dashed lines are 1 : 1.

critical parameters, is important for improving the NH_3 concentration estimation.

6.2 Global modeling results

While bidirectional exchange of NH_3 has previously been implemented in regional models (e.g., Bash et al., 2013; Zhang et al., 2010; Wichink Kruit et al., 2012), with the GEOS-Chem model we have the chance to evaluate NH_3 bidirectional exchange on global scales for the first time. The global distribution of NH_3 gross emissions in both BASE and BIDI cases, as well as their differences, are shown in Fig. 13. Generally, bidirectional exchange decreases NH_3 emissions in the Northern Hemisphere and increases NH_3 gross emissions in the Southern Hemisphere in April and October. Total NH_3 emissions in the Northern Hemisphere decrease by 22.6 % in April and 7.8 % in October. In July, bidirectional exchange increases NH_3 emissions in most places (7.1 % globally), except China and India. As evident from the figure, the differences in many places throughout the globe are very slight. With positive and negative differences, the global mean and median of the changes are quite small (for example, the mean and median differences in July are $-0.02 \text{ Gg month}^{-1}$ and 0, respectively). However, there are areas where the differences deviate significantly from 0 (for example the standard deviation of the difference in July is $3.76 \text{ Gg month}^{-1}$ in China). We thus focus our discussion on

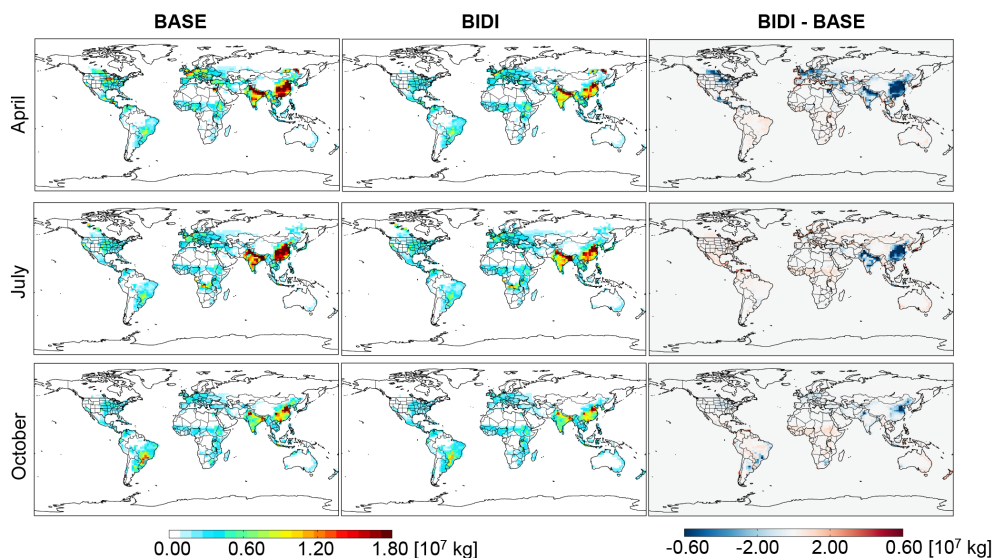


Figure 13. Global distribution of ammonia gross emissions from GEOS-Chem with (BIDI) and without (BASE) bidirectional exchange and their differences in April, July, and October of 2008. The total emissions in the BIDI case are the sum of upward fluxes from soil and vegetation from the bidirectional exchange and emissions from all other sources except fertilizers.

the range of differences in particular regions that are evident from Fig. 13. Significant decreases in NH₃ emissions in the BIDI case occur in southeastern China and northern India in all 3 months. The magnitudes of the decreases can be up to 18.4 Gg month⁻¹ in China and 16.5 Gg month⁻¹ in India in July. Total NH₃ emissions in China decrease by 43.6 % in April, 31.4 % in July, and 24.7 % in October. Total NH₃ emissions in India decrease by 28.8 % in April, 22.8 % in July, and 7.2 % in October. There are also large decreases of total NH₃ emissions in the USA, Mexico, and Europe in April of up to 6.5 Gg month⁻¹.

The changes of NH₃ gross emissions between BASE and BIDI cases can be seen more directly from the comparison of fertilizer emissions in the BASE case with those in the BIDI case. In Fig. 14, we show the global distribution of NH₃ fertilizer emissions in the BASE and BIDI cases. In the BIDI case, the fertilizer emissions are the upward fluxes from soil and vegetation from bidirectional exchange. The third column is the NH₃ emissions from all other sources except fertilizers in April, July, and October of 2008. In the BASE case, fertilizer emissions have peak values in eastern China and middle-east Asia and much smaller values elsewhere. Fertilizer emissions in the BIDI case increase in many places where there are no or near 0 values in the BASE case. In the BIDI case, the fertilizer emissions distribution is much more homogeneous. As we described in Sect. 6.1, fertilizer emissions are lower in the BIDI case under cool spring and fall time conditions due to the temperature effects on NH₃ emissions and storage in the soil ammonium pool. The deposition and re-emission processes in bidirectional exchange model thus extend the effect of NH₃ emissions from fertilizers. There are obvious trends that fertilizer emissions in the

Northern Hemisphere are larger than those in the Southern Hemisphere in April and July, and fertilizer emissions in the Southern Hemisphere are larger than those in the Northern Hemisphere in October. The global amount of NH₃ fertilizer emissions is 27.8 % of total emissions from all sources in the BASE case and 12.8 % in the BIDI case in April. Figure 15 shows the percentage of emissions from fertilizers in BIDI case in the global simulations. BIDI fertilizers contribute more to gross emissions in July than in other months in the Northern Hemisphere, which again demonstrates the delayed effect of fertilizer NH₃ (mostly applied in the spring-time) in the BIDI model.

Figure 16 shows the global distribution of NH₃ monthly surface concentrations in the BASE and BIDI cases and their differences in April, July, and October. Although bidirectional exchange changes NH₃ concentrations slightly throughout the globe (mean and median values of the changes are all nearly 0 in all 3 months), significant changes still exist in many places. In general, bidirectional exchange increases NH₃ concentrations in July by up to 3.9 ppb. It decreases NH₃ concentrations in the Northern Hemisphere (up to 27.6 ppb) and increases NH₃ concentrations in the Southern Hemisphere (up to 4.2 ppb) in April and October. Significant decreases of NH₃ concentrations occur in China in all 3 months with up to 20.6 ppb in April, 12.8 ppb in July, and 15.7 ppb in October. Paulot et al. (2014) indicated the MASAGE NH₃ emissions, which we use in this study, were higher than the bottom-up NH₃ emissions from Huang et al. (2012) in China in April and July and similar to the emissions from Streets et al. (2003) in April, July, and October. Over-estimation of NH₃ surface concentrations in GEOS-Chem in China is found in Wang et al. (2013) when using NH₃ emis-

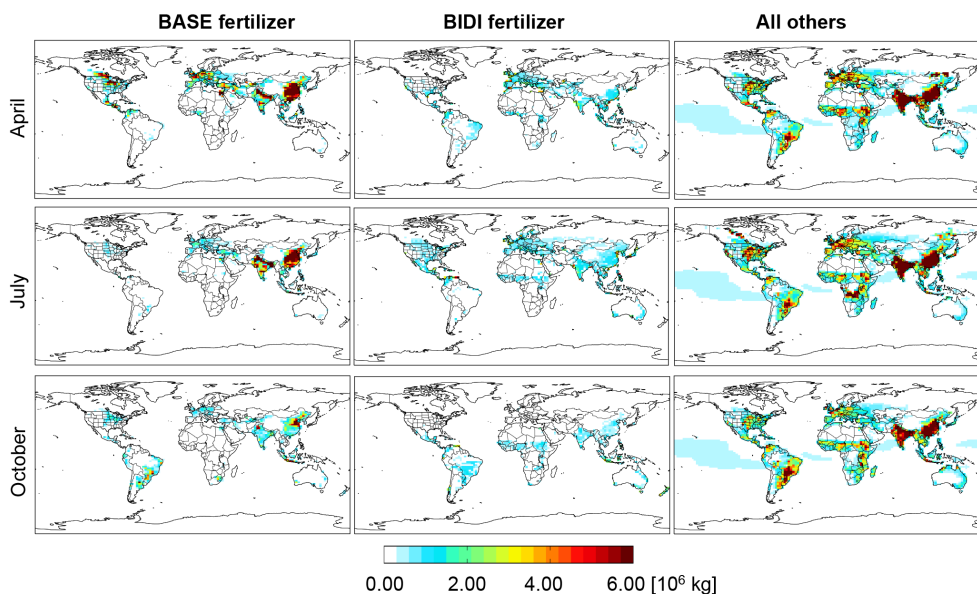


Figure 14. Global distribution of original ammonia fertilizer emissions in BASE case (BASE fertilizer), upward flux from soil and vegetation in BIDI case (BIDI fertilizer), and ammonia emissions from all other sources except fertilizers (all others) in April, July, and October of 2008.

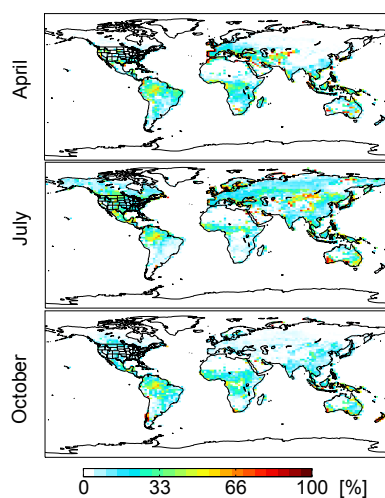


Figure 15. Percentage of gross emissions owing to fertilizer in the global BIDI case in April, July, and October of 2008.

sions from Streets et al. (2003), leading to an overestimation of nitrate aerosol concentrations in China. Observations from the Infrared Atmospheric Sounding Interferometer (IASI) remote sensing instrument have discrepancies over China with NH_3 concentrations in GEOS-Chem (Kharol et al., 2013; Clarisse et al., 2009) that may in part be improved by the impacts of bidirectional exchange. However, observations from TES show NH_3 concentrations in GEOS-Chem (with NH_3 emissions from Streets et al., 2003) are underestimated in many places of the globe including China (Shephard et al., 2011). We must note that the lower NH_3 concentrations presented here are daily averages, while IASI and TES data are

for a particular hour of the day. The changes in the emissions profile may reduce the model underestimate against the satellite observations while decreasing the mean NH_3 concentrations. However, the ability of remote sensing instruments on satellites in low-earth orbits to observe the impact of bidirectional exchange on NH_3 concentrations is limited compared to observations from potential future geostationary measurements (Zhu et al., 2015).

6.3 Wet deposition evaluation (global and USA)

We compare the model NH_4^+ wet deposition to in situ observations in several regions of the world using NTN for the continental USA, CAPMoN for Canada, EMEP for Europe, and EANET for eastern Asia; see Fig. 17. For the model NH_4^+ wet deposition, we also include the model NH_3 wet deposition since NH_4^+ wet deposition from in situ observations includes precipitated NH_3 . Since there are biases in the modeled precipitation, we scale the model wet deposition by multiplying the modeled deposition by the ratio of the observed to modeled precipitation, $\text{Flux}_{\text{model}} \cdot \left(\frac{P_{\text{obs}}}{P_{\text{model}}}\right)^{0.6}$, following the correction method in Paulot et al. (2014). We only include observations that have $0.25 < \frac{P_{\text{obs}}}{P_{\text{model}}} < 4$ to limit the effect of this correction (Paulot et al., 2014), and we also exclude observations which are beyond 3 times the standard deviation of observed NH_4^+ wet deposition to avoid outliers.

In general, the GEOS-Chem model underestimates NH_4^+ wet deposition throughout the world in the BASE case. Large increases in NH_4^+ wet deposition in the BIDI cases are found in the USA, Canada, and Europe in July (up to $6.31 \text{ kg ha}^{-1} \text{ yr}^{-1}$). The slopes of the regression line when compared to observations increase by 37.9% in the USA,

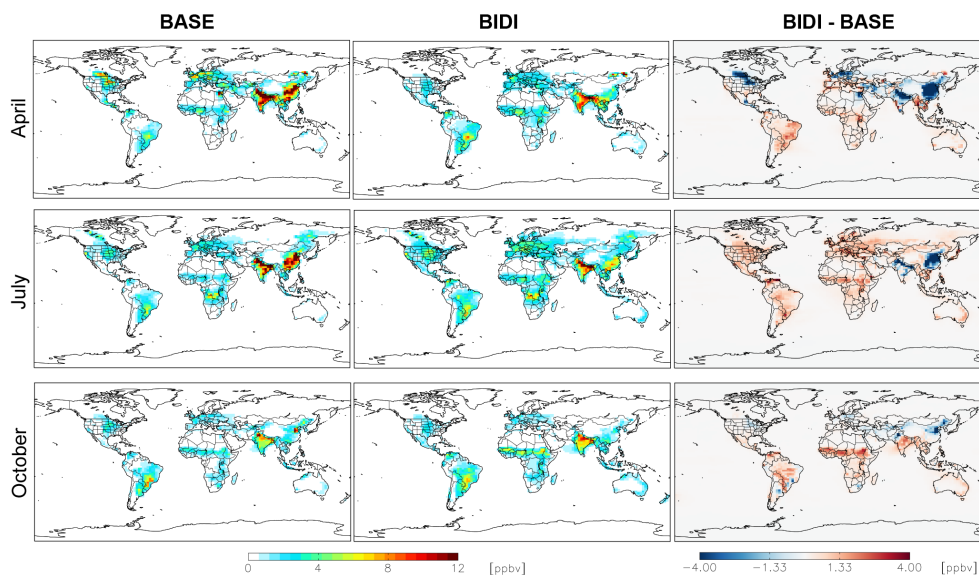


Figure 16. Global distribution of ammonia concentration at surface level of GEOS-Chem with (BIDI) and without (BASE) bidirectional exchange and their differences in April, July, and October of 2008.

54.9 % in Canada, and 17.7 % in Europe in the BIDI cases in July, all becoming closer to unity. However, the bidirectional exchange increases the RMSE by 64.3 % in the USA, 37.2 % in Canada, and 36.0 % in Europe.

Bidirectional exchange does not impact the NH_4^+ wet deposition much in April and October. It decreases NH_4^+ wet deposition slightly (up to $3.77 \text{ kg ha}^{-1} \text{ yr}^{-1}$ in Europe) at most of the observation locations in the USA, Canada, and Europe in April. The slopes decrease by 14.3 % in the USA, 6.8 % in Canada, and 12.3 % in Europe. Bidirectional exchange decreases the NMB by 46.4 % in the USA, 37.6 % in Europe in April, but increases the NMB by 28.3 % in Canada, and 11.6 % in eastern Asia. In October, bidirectional exchange increases NH_4^+ wet deposition slightly at most of the observation locations (up to $3.85 \text{ kg ha}^{-1} \text{ yr}^{-1}$). The changes in RMSE between BASE and BIDI cases are small, less than 10 %.

The overall differences of NH_4^+ wet deposition between the BASE and BIDI cases are generally small (from -4.95 to $6.31 \text{ kg ha}^{-1} \text{ yr}^{-1}$), even when the differences in NH_3 emissions are substantial. For example, NH_3 emissions differences between the BASE and BIDI range from -61.2 to $1.16 \text{ kg ha}^{-1} \text{ yr}^{-1}$ in China in April with bidirectional exchange, but changes in NH_4^+ wet deposition are not very large (from -4.95 to $2.52 \text{ kg ha}^{-1} \text{ yr}^{-1}$). While implementing NH_3 bidirectional exchange leads to improvements in some regions and seasons, it does not uniformly reduce error in model estimation of NH_4^+ wet deposition.

6.4 Adjoint sensitivity analysis

6.4.1 Global adjoint sensitivities

In Sect. 5.3, we demonstrated the accuracy of the sensitivities calculated using the adjoint of the GEOS-Chem bidirectional model. In this section, we present the adjoint sensitivities of NH_3 surface concentrations with respect to the important parameters in the bidirectional model. Figure 18 shows the adjoint sensitivities of NH_3 surface concentration with respect to the scaling factors for the soil pH (left) and for the fertilizer application rate (right) in April, July, and October 2008. The sensitivities with respect to both parameters are always positive throughout the globe. Sensitivities of NH_3 to fertilizer application rate are positive as excess fertilizer application will increase the NH_3 soil emission potential. Sensitivities of NH_3 to soil pH are also positive as low H^+ concentrations in soil (high soil pH) increases dissociation of NH_4^+ to NH_3 , thereby increasing the potential for volatilization of NH_3 .

The relationship between NH_3 concentration and soil pH is stronger during the growing season since more ammonium is in the soil pool. Slight changes in pH may have large impacts on the amount of NH_3 emitted from soil and further induce large differences in NH_3 surface concentrations. As we can see in the left column of Fig. 18, the sensitivities of NH_3 surface concentrations with respect to soil pH scaling factors are larger in the Northern Hemisphere than those in the Southern Hemisphere in April and July and less in the Northern Hemisphere than those in the Southern Hemisphere in October, since the growing seasons are in April in the Northern Hemisphere and in October in the Southern Hemisphere. Large sensitivities in July in the Northern

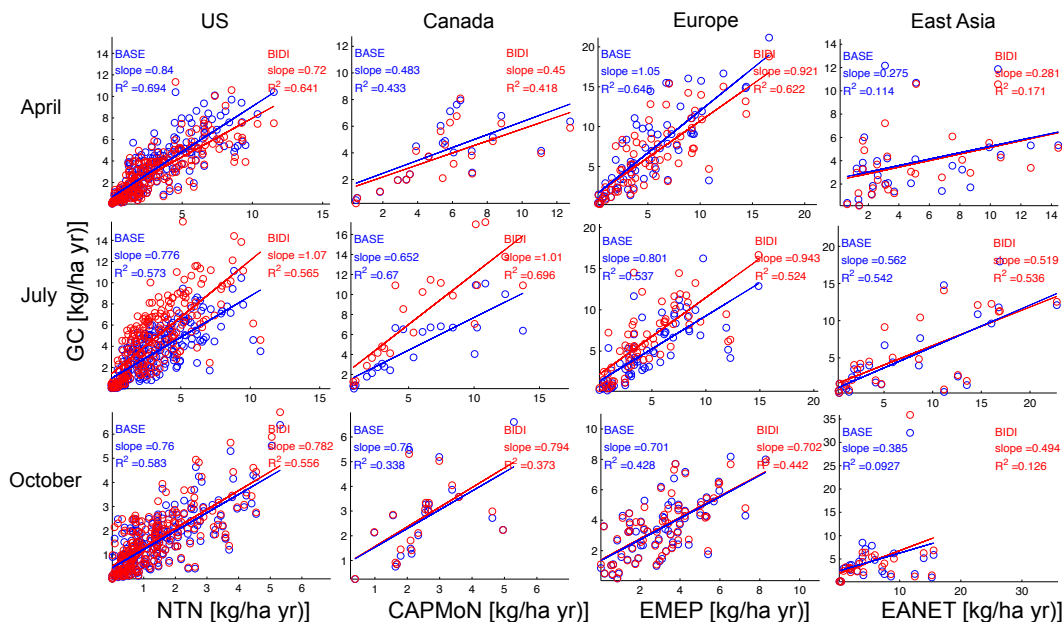


Figure 17. Comparisons of GEOS-Chem modeled NH₄⁺ wet deposition in BASE (blue) and BIDI (red) cases with in situ observations in the USA (first column), Canada (second column), Europe (third column), and eastern Asia (fourth column) in April (first row), July (second row), and October (third row) of 2008. The y axis represents the model values, and the x axis represents observations from NTN (for USA), CAPMoN (for Canada), EMEP (for Europe), and EANET (for eastern Asia). R^2 is the square of the correlation coefficient.

Hemisphere are due to ammonium in the soil pool accumulated from CAFO emissions via deposition. However, some caution is warranted in interpreting the seasonality of these sensitivities, as our model does not include any seasonal variations in soil pH. Seasonal variability of soil pH is driven by fertilizer rate, timing of fertilizer application, root and bacterial activity, soil moisture, organic matter, and salt levels (Murdoch and Call, 2006). Soil pH is observed to be highest at or near mid-winter and lowest at late summer (Slattery and Ronnfeldt, 1992). Variation of soil pH can be more than one unit from spring to fall (Angima, 2010); thus the uncertainty in the constant annual soil pH used here could be about 20 % owing to neglecting seasonality.

The relationship between NH₃ concentration and fertilizer application rate is also seasonally dependent. The seasonal trends of sensitivities of NH₃ to fertilizer application rate are similar to sensitivities of NH₃ to soil pH. Larger sensitivities appear in places with lower fertilizer application rates than those with plenty of fertilizer. For example, the largest fertilizer application rates appear in southeast China, northwest Europe and northern India in April, and sensitivities are nearly 0 in each of these locations. That the magnitude of the fertilizer application rates itself is an important factor in determining the sensitivities of NH₃ concentration to the fertilizer application rate is indicative of the nonlinear relationship introduced by treatment of bidirectional exchange.

Through investigating the sensitivities of NH₃ surface concentration to the soil pH and the fertilizer application rate, we know that NH₃ surface concentrations are very sensitive

to these parameters in many places of globe. We also find that NH₃ surface concentrations are more sensitive to soil pH than fertilizer application rate in general. In addition to the adjoint sensitivity analysis of NH₃ concentrations to the soil pH and the fertilizer application rate, it is also interesting to know the ranking of sensitivities of NH₃ concentrations with respect to other parameters, such as NH₃ concentrations at compensation points (C_c , C_{st} , C_g), NH₃ emission potentials (Γ_g , Γ_{st}), and resistances (R_a , R_{inc} , R_{soil} , R_g , R_{st} , R_{bg} , R_w). Knowledge of the sensitivity of NH₃ concentrations with respect to these parameters may help improve the model estimation of the spatial and temporal distributions as well as the magnitudes of NH₃ concentrations.

6.4.2 Comparison to in situ NH₃ with adjusted BIDI parameters

Based on the adjoint sensitivity analysis we have shown above and forward sensitivity analysis for all the parameters mentioned above (results not shown), we know that soil pH is one of the most critical parameters in the GEOS-Chem bidirectional exchange model. It is interesting to explore to what extent biases in the modeled NH₃ concentrations may be explained by uncertainties in the parameters of the bidirectional model, rather than, e.g., revising livestock NH₃ emissions. To test this, we increase the soil pH value by a factor of 1.1, since uncertainties of seasonal soil pH are about 20 %. As expected, the NH₃ surface concentrations generally increase over the globe (e.g., up to 3.4 ppb in April). Large increases

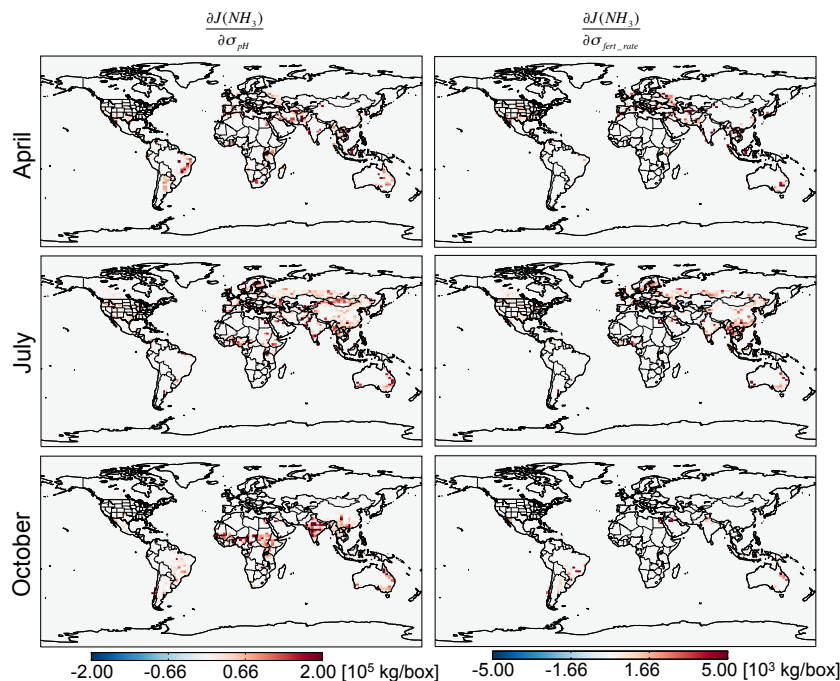


Figure 18. The adjoint sensitivities of NH_3 surface level concentration with respect to soil pH scaling factor (left) and fertilizer application rate scaling factor (right) in April, July, and October of 2008. Note that sensitivities in the left and right columns have different scales.

occur in places with large sensitivities to soil pH (Fig. 18, upper left). NH_3 concentrations are underestimated in the model in comparison to the AMoN observations in the USA. They are also underestimated in many parts of globe in comparison to TES observations (Shephard et al., 2011). With this adjustment to soil pH, the discrepancy between TES observations and the model in upper levels of the boundary layer may potentially be reduced in regions where GEOS-Chem NH_3 is underestimated before the growing seasons and overestimated after the growing seasons. Slight increases in NH_3 surface concentrations are found throughout the USA as NH_3 is not very sensitive to soil pH in the USA (see Fig. 18). Thus, this adjustment does not improve the comparison to AMoN observations in the USA.

In this study, we did not consider the adjustment of soil pH in agricultural areas by the farmers who limit the soil pH in a certain range to improve crop yield (Haynes and Naidu, 1998). However, no significant changes in the modeled surface NH_3 concentrations occur with bidirectional exchange when we limit the soil pH in the agricultural areas between 5.5 and 6.5 (generally less than 1 ppb over the globe, up to 3.4 ppb in India), since sensitivities are not very strong in the agricultural areas (see left column of Fig. 18).

Small differences between bidirectional and unidirectional fluxes in the USA are also indicated in Dennis et al. (2013), wherein sensitivity tests were performed varying the soil emission potential (Γ_g , a parameter which includes both soil pH and fertilizer application rate) in CMAQ. It was found that the impact on total N deposition at continental scales

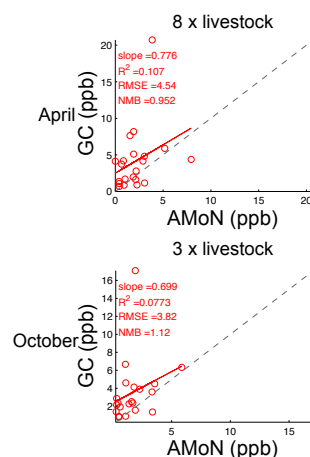


Figure 19. Comparison of NH_3 surface concentrations from GEOS-Chem with bidirectional exchange to AMoN observations. The livestock emissions in the model are increased by a factor of 6 in April and 3 in October.

was generally small ($< 5\%$), with very few ($< 10\%$) grid cells having differences up to 20%.

From Zhu et al. (2013), we know that the underestimation of NH_3 emissions in the unidirectional model can be as much as a factor of 9 in the USA. We also notice that NH_3 may not change much when fertilizer emissions increase a lot in regions such as midwest USA and northern Australia (see Figs. 14 and 16). Thus, low emissions from other sources,

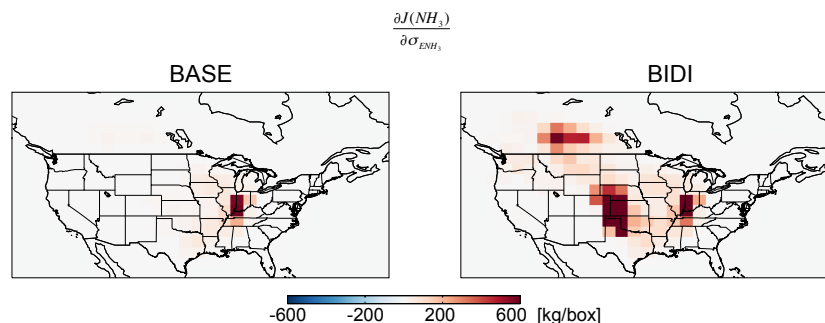


Figure 20. The adjoint sensitivities of NH₃ surface level concentration at 88° W, 40° N with respect to NH₃ anthropogenic emission scaling factor at all grid cells in both BASE (left) and BIDI (right) cases in April 2008.

such as livestock, may be a big part of the reason for underestimating NH₃ concentrations in the bidirectional exchange model. To better understand this, we also test increasing NH₃ livestock emissions by a factor of 8 in April and 3 in October as NH₃ concentrations are generally underestimated by around 8 and 3 times (Fig. 10) compared to AMoN observations in April and October, respectively. These adjustments bring the NH₃ concentrations into a much better agreement with the magnitude of AMoN observations; see Fig. 19. However, uniformly increasing the livestock emissions does not well represent the NH₃ spatial distribution with the AMoN observations (correlations of model and observation are very low). Overall, treatment of bidirectional exchange can improve our understanding of NH₃ emissions from fertilizers, but this alone may not improve estimation of NH₃ concentrations, NH₄⁺ wet depositions, and nitrate aerosol concentrations. Additional work including bidirectional exchange in NH₃ inverse modeling is needed, as large underestimates in NH₃ primary sources exist in the model and simply applying the scheme to optimized emissions from inverse modeling can not capture well the spatial variability of NH₃ concentrations that are the responses of both bidirectional exchange processes and emissions.

6.4.3 Spot sensitivity analysis

Here we investigate to what extent bidirectional exchange increases the NH₃ lifetime, which is a critical issue for controlling nitrogen deposition and PM_{2.5} formation. Through the adjoint method, we are able to assess source contributions to model estimates in particular response regions (e.g., Lee et al., 2014). In Fig. 20, we show the adjoint sensitivity of NH₃ surface concentration at a single location (88° W, 40° N) with respect to the NH₃ anthropogenic emissions at all grid cells in April 2008. In the BASE case (left panel), the NH₃ surface concentration is most sensitive to the emissions from the same grid cell and is less sensitive to the emissions from surrounding grid cells. With the bidirectional exchange (right panel), the NH₃ concentration is sensitive to the emissions from a much wider range, which extends all the way

to Canada. Some of the sensitivities are very strong even though they are a long distance away from the location of the NH₃ concentration under consideration. The deposition and re-emission processes in the bidirectional exchange extends the spatial range of influence of NH₃ emissions and, in effect, the NH₃ lifetime. Thus, modeled NH₃ concentrations in Illinois can be impacted by the emissions from Kansas or even from Canada.

7 Conclusions

In this study, we have considered a more detailed, process-level treatment of NH₃ sources in a global chemical transport model (GEOS-Chem) and evaluated the model behavior in terms of biases in estimated NH₃, nitrate, and NH₄⁺ wet deposition and the factors driving these processes in the model. First, we update the diurnal variability of NH₃ livestock emissions. In general, by implementing this diurnal variability scheme, the global NH₃ concentrations, nitrate aerosol concentrations, and nitrogen deposition all decrease. The largest decreases always occur in southeastern China and northern India. More NH₃ from livestock emitted in the daytime largely decreases the NH₃ surface concentrations in the night and increases concentrations during the day, which is more conducive to export of NH₃.

We have also developed bidirectional exchange of NH₃ and its adjoint in the GEOS-Chem model. Bidirectional exchange generally increases NH₃ gross emissions in most parts of the USA and most places around the globe in July, except China and India. These are mainly due to the NH₃ re-emissions from the ammonium soil pool that accumulates ammonium from previous months. Bidirectional exchange generally decreases NH₃ gross emissions in the USA in April and October. On a global scale, bidirectional exchange decreases NH₃ gross emissions in the Northern Hemisphere in April and October and increases NH₃ gross emissions in the Southern Hemisphere. During the growing seasons, the ammonium soil pool preserves ammonia/ammonium in the soil rather than emitting it directly after fertilizer application.

Bidirectional exchange increases monthly NH₃ surface concentrations throughout the world in July, which improves comparison to the AMoN observations in the USA. It decreases NH₃ surface concentrations in the Northern Hemisphere and increases NH₃ concentrations in the Southern Hemisphere in April and October. Bidirectional exchange does not have a large impact on model biases in nitrate aerosol, which are likely owing to overestimated nitric acid concentration (Heald et al., 2012). However, with the deposition and re-emission of NH₃ inherent in bidirectional exchange, NH₃ can be impacted by sources from a much greater distance, which is a critical issue when considering strategies for controlling nitrogen deposition and PM_{2.5} formation.

Bidirectional exchange largely increases NH₄⁺ wet deposition in the USA, Canada, and Europe in July but slightly decreases NH₄⁺ wet deposition in April and has little impact in October. The overall differences of NH₄⁺ wet deposition between the BASE and BIDI cases are generally small, even when the differences in NH₃ fertilizer emissions are large. While observations of wet deposition have been used to constrain NH₃ sources in previous works (Gilliland et al., 2003, 2006; Zhang et al., 2012; Paulot et al., 2014), this data set does not appear sufficient to provide constraints on model treatment of bidirectional exchange. Moreover, as the in situ measurements used here are limited in space and time, the comparisons between model and measurements only represents the ability of bidirectional parameterization at these specific spatial (100s of km) and temporal (monthly) scales; more pronounced impacts may occur at finer scales.

Using the adjoint of bidirectional exchange, we investigate the spatial and seasonal dependency of NH₃ surface concentrations in the GEOS-Chem model on the soil pH and fertilizer application rate, which are themselves uncertain. Soil pH is known to be seasonally variable. Updating the soil pH with seasonal variability would impact the results of bidirectional exchange across wide regions of globe. However, updating the soil pH with seasonal variability does not seem sufficient to improve comparison with in situ observations in the USA, as primary sources are likely underestimated by a factor of 3 or more. Further, uniformly increasing the emissions from primary sources degrades the spatial variability of simulated NH₃.

Overall, bidirectional exchange largely extends the lifetime of NH₃ in the atmosphere via deposition and re-emission processes. This model provides a better fundamental description of NH₃ emissions from fertilizers. However, implementing bidirectional exchange does not uniformly improve estimation of NH₃ concentrations, NH₄⁺ wet deposition, and nitrate aerosol concentrations. Domain-wide adjustments to soil pH or livestock emissions do not improve the model comparison to the full suite of measurements from different platforms, locations, and seasons considered here. Thus, incorporating bidirectional exchange in an in-

verse model is required in future work to correct the low biases in NH₃ primary sources without over adjusting these sources to account for model error from neglecting bidirectional exchange processes. Measurements from recent (Shepherd and Cady-Pereira, 2015) or future (Zhu et al., 2015) remote sensing platforms will be of value for such endeavors.

Acknowledgements. This work is supported by NASA grants NNX09AN77G and NNX10AG63G and EPA STAR award RD834559. While this manuscript has been reviewed by the Environmental Protection Agency and approved for publication, it may not reflect official agency views or policies.

Edited by: L. Ganzeveld

References

- Angima, S.: Measuring Soil pH, Oregon State University Small Farms Program, 2010.
- Bash, J., Walker, J., Katul, G., Jones, M., Nemitz, E., and Robarge, W.: Estimation of in-canopy ammonia sources and sinks in a fertilized Zea Mays field, *Environ. Sci. Technol.*, 44, 1683–1689, 2010.
- Bash, J. O., Cooter, E. J., Dennis, R. L., Walker, J. T., and Pleim, J. E.: Evaluation of a regional air-quality model with bidirectional NH₃ exchange coupled to an agroecosystem model, *Biogeosciences*, 10, 1635–1645, doi:10.5194/bg-10-1635-2013, 2013.
- Bey, I., Jacob, D. J., Yantosca, R. M., Logan, J. A., Field, B. D., Fiore, A. M., Li, Q. B., Liu, H. G. Y., Mickley, L. J., and Schultz, M. G.: Global modeling of tropospheric chemistry with assimilated meteorology: Model description and evaluation, *J. Geophys. Res.-Atmos.*, 106, 23073–23095, 2001.
- Bouwman, A. F., Lee, D. S., Asman, W. A. H., Dentener, F. J., VanderHoek, K. W., and Olivier, J. G. J.: A global high-resolution emission inventory for ammonia, *Global Biogeochem. Cy.*, 11, 561–587, 1997.
- Ciais, P., Sabine, C., Bala, G., Bopp, L., Brovkin, V., Canadell, J., Chhabra, A., DeFries, R., Galloway, J., Heimann, M., Jones, C., Quéré, C. L., Myneni, R., Piao, S., and Thornton, P.: Carbon and Other Biogeochemical Cycles, in *Climate Change 2013, The Physical Science Basis, Contribution of Working Group I to the Fifth Assessment Report*, 465–570, 2013.
- Clarisse, L., Clerbaux, C., Dentener, F., Hurtmans, D., and Coheur, P. F.: Global ammonia distribution derived from infrared satellite observations, *Nat. Geosci.*, 2, 479–483, doi:10.1038/Ngeo551, 2009.
- Cooter, E. J., Bash, J. O., Walker, J. T., Jones, M., and Robarge, W.: Estimation of NH₃ bi-directional flux from managed agricultural soils, *Atmos. Environ.*, 44, 2107–2115, doi:10.1016/j.atmosenv.2010.02.044, 2010.
- Crouse, D. L., Peters, P. A., van Donkelaar, A., Goldberg, M. S., Villeneuve, P. J., Brion, O., Khan, S., Atari, D. O., Jerrett, M., Pope, C. A., Brauer, M., Brook, J. R., Martin, R. V., Stieb, D., and Burnett, R. T.: Risk of Non accidental and Cardiovascular Mortality in Relation to Long-term Exposure to Low Concentrations of Fine Particulate Matter: A Canadian National-

- Level Cohort Study, *Environ. Health Persp.*, 120, 708–714, doi:10.1289/ehp.1104049, 2012.
- Dennis, R., Schwede, D., Bash, J., Pleim, J., Walker, J., and Foley, K.: Sensitivity of continental United States atmospheric budgets of oxidized and reduced nitrogen to dry deposition parametrizations, *Philos. T. Roy. Soc. B*, 368, 20130124, doi:10.1098/rstb.2013.0124, 2013.
- Elbern, H., Schmidt, H., and Ebel, A.: Variational data assimilation for tropospheric chemistry modeling, *J. Geophys. Res.-Atmos.*, 102, 15967–15985, 1997.
- Elbern, H., Schmidt, H., Talagrand, O., and Ebel, A.: 4D-varational data assimilation with an adjoint air quality model for emission analysis, *Environ. Modell. Softw.*, 15, 539–548, 2000.
- Fisher, M. and Lary, D. J.: Lagrangian four-dimensional variational data assimilation of chemical species, *Q. J. Roy. Meteorol. Soc.*, 121, 1681–1704, 1995.
- Galloway, J. N., Townsend, A. R., Erisman, J. W., Bekunda, M., Cai, Z. C., Freney, J. R., Martinelli, L. A., Seitzinger, S. P., and Sutton, M. A.: Transformation of the nitrogen cycle: Recent trends, questions, and potential solutions, *Science*, 320, 889–892, doi:10.1126/Science.1136674, 2008.
- Gilliland, A. B., Dennis, R. L., Roselle, S. J., and Pierce, T. E.: Seasonal NH₃ emission estimates for the eastern United States based on ammonium wet concentrations and an inverse modeling method, *J. Geophys. Res.-Atmos.*, 108, 4477, doi:10.1029/2002JD003063, 2003.
- Gilliland, A. B., Appel, K. W., Pinder, R. W., and Dennis, R. L.: Seasonal NH₃ emissions for the continental United States: Inverse model estimation and evaluation, *Atmos. Environ.*, 40, 4986–4998, 2006.
- Haynes, R. and Naidu, R.: Influence of lime, fertilizer and manure applications on soil organic matter content and soil physical conditions: a review, *Nutr. Cycl. Agroecosys.*, 51, 123–137, doi:10.1023/A:1009738307837, 1998.
- Heald, C. L., Collett Jr., J. L., Lee, T., Benedict, K. B., Schwandner, F. M., Li, Y., Clarisse, L., Hurtmans, D. R., Van Damme, M., Clerbaux, C., Coheur, P.-F., Philip, S., Martin, R. V., and Pye, H. O. T.: Atmospheric ammonia and particulate inorganic nitrogen over the United States, *Atmos. Chem. Phys.*, 12, 10295–10312, doi:10.5194/acp-12-10295-2012, 2012.
- Henze, D. K., Hakami, A., and Seinfeld, J. H.: Development of the adjoint of GEOS-Chem, *Atmos. Chem. Phys.*, 7, 2413–2433, doi:10.5194/acp-7-2413-2007, 2007.
- Henze, D. K., Seinfeld, J. H., and Shindell, D. T.: Inverse modeling and mapping US air quality influences of inorganic PM_{2.5} precursor emissions using the adjoint of GEOS-Chem, *Atmos. Chem. Phys.*, 9, 5877–5903, doi:10.5194/acp-9-5877-2009, 2009.
- Huang, X., Song, Y., Li, M., Li, J., Huo, Q., Cai, X., Zhu, T., Hu, M., and Zhang, H.: A high-resolution ammonia emission inventory in China, *Global Biogeochem. Cy.*, 26, GB1030, doi:10.1029/2011GB004161, 2012.
- Hudman, R. C., Moore, N. E., Mebust, A. K., Martin, R. V., Russell, A. R., Valin, L. C., and Cohen, R. C.: Steps towards a mechanistic model of global soil nitric oxide emissions: implementation and space based-constraints, *Atmos. Chem. Phys.*, 12, 7779–7795, doi:10.5194/acp-12-7779-2012, 2012.
- Kharol, S. K., Martin, R. V., Philip, S., Vogel, S., Henze, D. K., Chen, D., Wang, Y., Zhang, Q., and Heald, C. L.: Persistent sensitivity of Asian aerosol to emissions of nitrogen oxides, *Geophys. Res. Lett.*, 40, 1021–1026, doi:10.1002/grl.50234, 2013.
- Kopacz, M., Jacob, D. J., Fisher, J. A., Logan, J. A., Zhang, L., Megretskaiya, I. A., Yantosca, R. M., Singh, K., Henze, D. K., Burrows, J. P., Buchwitz, M., Khlystova, I., McMillan, W. W., Gille, J. C., Edwards, D. P., Eldering, A., Thouret, V., and Nedelec, P.: Global estimates of CO sources with high resolution by adjoint inversion of multiple satellite datasets (MOPITT, AIRS, SCIAMACHY, TES), *Atmos. Chem. Phys.*, 10, 855–876, doi:10.5194/acp-10-855-2010, 2010.
- Lamarque, J.-F., Kyle, G., Meinshausen, M., Riahi, K., Smith, S., van Vuuren, D., Conley, A., and Vitt, F.: Global and regional evolution of short-lived radiatively-active gases and aerosols in the Representative Concentration Pathways, *Climatic Change*, 109, 191–212, doi:10.1007/s10584-011-0155-0, 2011.
- Langridge, J. M., Lack, D. A., Brock, C. A., Bahreini, R., Middlebrook, A. M., Neuman, J. A., Nowak, J. B., Perring, A. E., Schwarz, J. P., Spackman, J. R., Holloway, J. S., Pollack, I. B., Ryerson, T. B., Roberts, J. M., Warneke, C., de Gouw, J., Trainer, M. K., and Murphy, D. M.: Evolution of aerosol properties impacting visibility and direct climate forcing in an ammonia-rich urban environment, *J. Geophys. Res.*, 117, D00V11, doi:10.1029/2011JD017116, 2012.
- Lee, H.-M., Henze, D., Alexander, B., and Murray, L.: Investigating the sensitivity of surface-level nitrate seasonality in Antarctica to primary sources using a global model, *Atmos. Environ.*, 89, 757–767, doi:10.1016/j.atmosenv.2014.03.003, 2014.
- Liao, H., Henze, D. K., Seinfeld, J. H., Wu, S., and Mickley, L. J.: Biogenic secondary organic aerosol over the United States: Comparison of climatological simulations with observations, *J. Geophys. Res.-Atmos.*, 112, D06201, doi:10.1029/2006JD007813, 2007.
- Liu, H. Y., Jacob, D. J., Bey, I., and Yantosca, R. M.: Constraints from Pb-210 and Be-7 on wet deposition and transport in a global three-dimensional chemical tracer model driven by assimilated meteorological fields, *J. Geophys. Res.*, 106, 12109–12128, 2001.
- Liu, X., Zhang, Y., Han, W., Tang, A., Shen, J., Cui, Z., Vitousek, P., Erisman, J. W., Goulding, K., Christie, P., Fangmeier, A., and Zhang, F.: Enhanced nitrogen deposition over China, *Nature*, 494, 459–462, doi:10.1038/nature11917, 2013.
- Malm, W. C., Schichtel, B. A., Pitchford, M. L., Ashbaugh, L. L., and Eldred, R. A.: Spatial and monthly trends in speciated fine particle concentration in the United States, *J. Geophys. Res.-Atmos.*, 109, D03306, doi:10.1029/2003jd003739, 2004.
- Martien, P. T. and Harley, R. A.: Adjoint sensitivity analysis for a three-dimensional photochemical model: Application to Southern California, *Environ. Sci. Technol.*, 40, 4200–4210, 2006.
- Matson, P. A., Naylor, R. L., and Ortiz-Monasterio, I.: Integration of environmental, agronomic, and economic aspects of fertilizer management, *Science*, 280, 112–115, 1998.
- Murdock, L. and Call, D.: *Managing Seasonal Fluctuations of Soil Tests*, University of Kentucky Cooperative Extension, 2006.
- Nemitz, E., Sutton, M. A., Schjoerring, J. K., Husted, S., and Wyers, G. P.: Resistance modelling of ammonia exchange above oilseed rape, *Agr. Forest Meteorol.*, 105, 405–425, 2000.
- Nemitz, E., Milford, C., and Sutton, M. A.: A two-layer canopy compensation point model for describing bi-directional

- biosphere-atmosphere exchange of ammonia, *Q. J. Roy. Meteor. Soc.*, 127, 815–833, 2001.
- Nowak, J. B., Neuman, J. A., Bahreini, R., Middlebrook, A. M., Holloway, J. S., McKeen, S. A., Parrish, D. D., Ryerson, T. B., and Trainer, M.: Ammonia sources in the California South Coast Air Basin and their impact on ammonium nitrate formation, *Geophys. Res. Lett.*, 39, L07804, doi:10.1029/2012GL051197, 2012.
- Park, R. J., Jacob, D., Field, B. D., Yantosca, R., and Chin, M.: Natural and transboundary pollution influences on sulfate-nitrate-ammonium aerosols in the United States: Implications for policy, *J. Geophys. Res.-Atmos.*, 109, D15204, doi:10.1029/2003JD004473, 2004.
- Paulot, F., Jacob, D. J., Pinder, R. W., Bash, J. O., Travis, K., and Henze, D. K.: Ammonia emissions in the United States, European Union, and China derived by high-resolution inversion of ammonium wet deposition data: Interpretation with a new agricultural emissions inventory (MASAGE_NH₃), *J. Geophys. Res.-Atmos.*, 119, 4343–4364, doi:10.1002/2013JD021130, 2014.
- Pinder, R. W., Adams, P. J., Pandis, S. N., and Gilliland, A. B.: Temporally resolved ammonia emission inventories: Current estimates, evaluation tools, and measurement needs, *J. Geophys. Res.-Atmos.*, 111, D16310, doi:10.1029/2005JD006603, 2006.
- Pinder, R. W., Walker, J. T., Bash, J. O., Cady-Pereira, K. E., Henze, D. K., Luo, M., Osterman, G. B., and Shephard, M. W.: Quantifying spatial and temporal variability in atmospheric ammonia with in situ and space-based observations, *Geophys. Res. Lett.*, 38, L04802, doi:10.1029/2010GL046146, 2011.
- Pleim, J. E., Bash, J. O., Walker, J. T., and Cooter, E. J.: Development and evaluation of an ammonia bidirectional flux parameterization for air quality models, *J. Geophys. Res.-Atmos.*, 118, 3794–3806, doi:10.1002/jgrd.50262, 2013.
- Pope, C. A., Ezzati, M., and Dockery, D. W.: Fine-particulate air pollution and life expectancy in the United States, *N. Engl. J. Med.*, 360, 376–386, 2009.
- Potter, P., Ramankutty, N., Bennett, E. M., and Donner, S. D.: Characterizing the spatial patterns of global fertilizer application and manure production, *Earth Interact.*, 14, 1–22, 2010.
- Puchalski, M. A., Sather, M. E., Walker, J. T., Lehmann, C. M., Gay, D. A., Mathew, J., and Robarge, W. P.: Passive ammonia monitoring in the United States: comparing three different sampling devices, *J. Environ. Monitor.*, 13, 3156–3167, 2011.
- Reiss, R., Anderson, E. L., Cross, C. E., Hidy, G., Hoel, D., McClellan, R., and Moolgavkar, S.: Evidence of health impacts of sulfate- and nitrate-containing particles in ambient air, *Inhal Toxicol.*, 19, 419–449, doi:10.1080/08958370601174941, 2007.
- Schiferl, L. D., Heald, C. L., Nowak, J. B., Holloway, J. S., Neuman, J. A., Bahreini, R., Pollack, I. B., Ryerson, T. B., Wiedinmyer, C., and Murphy, J. G.: An investigation of ammonia and inorganic particulate matter in California during the CalNex campaign, *J. Geophys. Res.-Atmos.*, 119, 1883–1902, doi:10.1002/2013JD020765, 2014.
- Shephard, M. W. and Cady-Pereira, K. E.: Cross-track Infrared Sounder (CrIS) satellite observations of tropospheric ammonia, *Atmos. Meas. Tech.*, 8, 1323–1336, doi:10.5194/amt-8-1323-2015, 2015.
- Shephard, M. W., Cady-Pereira, K. E., Luo, M., Henze, D. K., Pinder, R. W., Walker, J. T., Rinsland, C. P., Bash, J. O., Zhu, L., Payne, V. H., and Clarisse, L.: TES ammonia retrieval strategy and global observations of the spatial and seasonal variability of ammonia, *Atmos. Chem. Phys.*, 11, 10743–10763, doi:10.5194/acp-11-10743-2011, 2011.
- Slattery, W. and Ronnfeldt, G.: Seasonal variation of pH, aluminium, and manganese in acid soils from north-eastern Victoria, *Aust. J. Exp. Agr.*, 32, 1105–1112, 1992.
- Streets, D., Zhang, Q., Wang, L., He, K., Hao, J., Wu, Y., Tang, Y., and Carmichael, G.: Revisiting China's CO emissions after the Transport and Chemical Evolution over the Pacific (TRACE-P) mission: Synthesis of inventories, atmospheric modeling, and observations, *J. Geophys. Res.*, 111, D14306, doi:10.1029/2006JD007118, 2006.
- Streets, D. G., Bond, T. C., Carmichael, G. R., Fernandes, S. D., Fu, Q., Klimont, Z., Nelson, S. M., Tsai, N. Y., Wang, M. Q., Woo, J.-H., and Yarber, K. F.: An inventory of gaseous and primary aerosol emissions in Asia in the year 2000, *J. Geophys. Res.*, 108, 8809, doi:10.1029/2002JD003093, 2003.
- Sutton, M., Burkhardt, J., Guerin, D., Nemitz, E., and Fowler, D.: Development of resistance models to describe measurements of bi-directional ammonia surface-atmosphere exchange, *Atmos. Environ.*, 32, 473–480, 1998.
- Sutton, M. A., Nemitz, E., Erisman, J. W., Beier, C., Bahl, K. B., Cellier, P., de Vries, W., Cotrufo, F., Skiba, U., Di Marco, C., Jones, S., Laville, P., Soussana, J. F., Loubet, B., Twigg, M., Famulari, D., Whitehead, J., Gallagher, M. W., Neftel, A., Flechard, C. R., Herrmann, B., Calanca, P. L., Schjoerring, J. K., Daemmgen, U., Horvath, L., Tang, Y. S., Emmett, B. A., Tietema, A., Penuelas, J., Kesik, M., Brueggemann, N., Pilegaard, K., Vesala, T., Campbell, C. L., Olesen, J. E., Dragosits, U., Theobald, M. R., Levy, P., Mobbs, D. C., Milne, R., Viovy, N., Vuichard, N., Smith, J. U., Smith, P., Bergamaschi, P., Fowler, D., and Reis, S.: Challenges in quantifying biosphere-atmosphere exchange of nitrogen species, *Environ. Pollut.*, 150, 125–139, doi:10.1016/J.Envpol.2007.04.014, 2007.
- Van Damme, M., Clarisse, L., Heald, C. L., Hurtmans, D., Ngadi, Y., Clerbaux, C., Dolman, A. J., Erisman, J. W., and Coheur, P. F.: Global distributions, time series and error characterization of atmospheric ammonia (NH₃) from IASI satellite observations, *Atmos. Chem. Phys.*, 14, 2905–2922, doi:10.5194/acp-14-2905-2014, 2014.
- van der Werf, G. R., Randerson, J. T., Giglio, L., Collatz, G. J., Mu, M., Kasibhatla, P. S., Morton, D. C., DeFries, R. S., Jin, Y., and van Leeuwen, T. T.: Global fire emissions and the contribution of deforestation, savanna, forest, agricultural, and peat fires (1997–2009), *Atmos. Chem. Phys.*, 10, 11707–11735, doi:10.5194/acp-10-11707-2010, 2010.
- van Donkelaar, A., Martin, R. V., Leaitch, W. R., Macdonald, A. M., Walker, T. W., Streets, D. G., Zhang, Q., Dunlea, E. J., Jimenez, J. L., Dibb, J. E., Huey, L. G., Weber, R., and Andreae, M. O.: Analysis of aircraft and satellite measurements from the Intercontinental Chemical Transport Experiment (INTEX-B) to quantify long-range transport of East Asian sulfur to Canada, *Atmos. Chem. Phys.*, 8, 2999–3014, doi:10.5194/acp-8-2999-2008, 2008.
- Vestreng, V. and Klein, H.: Emission data reported to UNECE/EMEP. Quality assurance and trend analysis and Presentation of WebDab, Norwegian Meteorological Institute, Oslo, Norway, MSC-W Status Report, 2002.

- Walker, J. M., Philip, S., Martin, R. V., and Seinfeld, J. H.: Simulation of nitrate, sulfate, and ammonium aerosols over the United States, *Atmos. Chem. Phys.*, 12, 11213–11227, doi:10.5194/acp-12-11213-2012, 2012.
- Wang, Y., Zhang, Q. Q., He, K., Zhang, Q., and Chai, L.: Sulfate-nitrate-ammonium aerosols over China: response to 2000–2015 emission changes of sulfur dioxide, nitrogen oxides, and ammonia, *Atmos. Chem. Phys.*, 13, 2635–2652, doi:10.5194/acp-13-2635-2013, 2013.
- Wesely, M. L.: Parameterization of surface resistances to gaseous dry deposition in regional-scale numerical-models, *Atmos. Environ.*, 23, 1293–1304, 1989.
- Wichink Kruit, R. J., Schaap, M., Sauter, F. J., van Zanten, M. C., and van Pul, W. A. J.: Modeling the distribution of ammonia across Europe including bi-directional surface–atmosphere exchange, *Biogeosciences*, 9, 5261–5277, doi:10.5194/bg-9-5261-2012, 2012.
- Xu, X., Wang, J., Henze, D. K., Qu, W., and Kopacz, M.: Constraints on aerosol sources using GEOS-Chem adjoint and MODIS radiances, and evaluation with multisensor (OMI, MISR) data, *J. Geophys. Res.-Atmos.*, 118, 6396–6413, doi:10.1002/jgrd.50515, 2013.
- Yevich, R. and Logan, J. A.: An assessment of biofuel use and burning of agricultural waste in the developing world, *Global Biogeochem. Cy.*, 17, 1095, doi:10.1029/2002GB001952, 2003.
- Zhang, L., Wright, L. P., and Asman, W. A. H.: Bi-directional air-surface exchange of atmospheric ammonia: A review of measurements and a development of a big leaf model for applications in regional-scale air-quality models, *J. Geophys. Res.*, 115, D20310, doi:10.1029/2009JD013589, 2010.
- Zhang, L., Jacob, D. J., Knipping, E. M., Kumar, N., Munger, J. W., Carouge, C. C., van Donkelaar, A., Wang, Y. X., and Chen, D.: Nitrogen deposition to the United States: distribution, sources, and processes, *Atmos. Chem. Phys.*, 12, 4539–4554, doi:10.5194/acp-12-4539-2012, 2012.
- Zhu, L., Henze, D. K., Cady-Pereira, K. E., Shephard, M. W., Luo, M., Pinder, R. W., Bash, J. O., and Jeong, G.: Constraining U.S. ammonia emissions using TES remote sensing observations and the GEOS-Chem adjoint model, *J. Geophys. Res.-Atmos.*, 118, 3355–3368, doi:10.1002/jgrd.50166, 2013.
- Zhu, L., Henze, D. K., Bash, J. O., Cady-Pereira, K. E., Shephard, M. W., Luo, M., and Capps, S. L.: Sources and impacts of atmospheric NH₃: Current understanding and frontiers for modeling, measurements, and remote sensing in North America, *Current Pollution Reports*, 1, 95–116, doi:10.1007/s40726-015-0010-4, 2015.